'ANL-83-35

ANL-83-35

AML—83-35

OE84 025029

ELEVATED-TEMPERATURE, HIGH-CYCLE FATIGUE BEHAVIOR OF TYPE 316 STAINLESS STEEL

by

D. T. Raske and G. E. Korth

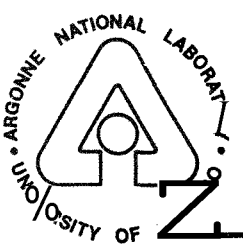

ARGONNE NATIONAL LABORATORY, ARGONNE, ILLINOIS

Operated by THE UNIVERSITY OF CHICAGO
for the U. S. DEPARTMENT OF ENERGY
under Contract W-31-109-Eng-38

DISCLAIMER

Distribution Category:
LMFBR—Structural Materials and
Design Engineering: Applied
Technology (UC-79Th)

ANL-83-35

ARGONNE NATIONAL LABORATORY
9700 South Cass Avenue
Argonne, Illinois 60439

ELEVATED-TEMPERATURE, HIGH-CYCLE FATIGUE BEHAVIOR OF TYPE 316 STAINLESS STEEL*

by

D. T. Raske and G. E. Korth**

July 1983

* Work performed under DOE B&R No. AF 15 40 10 3, Breeder Reactor Materials and Structures Task AN-1.3, Mechanical Properties Design Data.

**Idaho National Engineering Laboratory (EG&G Idaho, Inc.).

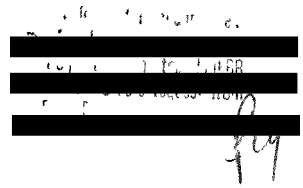

DISCLAIMER

TABLE OF CONTENTS

LIST OF FIGURES

LIST OF TABLES

ELEVATED-TEMPERATURE, HIGH-CYCLE FATIGUE BEHAVIOR OF TYPE 316 STAINLESS STEEL

by

D. T. Raske and G. E. Korth

ABSTRACT

This report presents the results of a study on the elevated-temperature high-cycle fatigue behavior of Type 316 stainless steel. The primary objective was to determine the 10^8-cycle endurance strain range at 593°C. Subsequently, other tests explored the effects of temperature, prior low-cycle fatigue damage, metallurgical variables, and weldments on this endurance strain limit. It was found that decreasing the test temperature to 482°C raised this strain limit by about 5%, and that limited amounts of prior low-cycle fatigue straining did not affect the strain limit. The endurance limit varies from heat to heat. Pretest thermal aging in sodium and use of as-welded all weld-metal specimens both lower this strain limit by about 8%. In the course of testing, it was found that the high-cycle fatigue behavior of this steel is very sensitive to grain size and to strain rate during the cyclic hardening phase. An increase in strain rate by a factor of 20 can increase the fatigue life by a factor of 7. Similarly, as the grain size decreases the fatigue life increases. Design curves derived from the baseline data at 482 and 593°C are discussed and compared with the existing ASME design curves.

I. INTRODUCTION

This report describes the results of a program to determine the elevated-temperature high-cycle fatigue behavior of Type 316 stainless steel. The primary objective of this study was to determine the in-air, 10^8-cycle endurance strain range at 593°C in support of the design of the upper core internal structure for the Clinch River Breeder Reactor Plant (CRBRP). Another objective was to investigate the effects of several key parameters on the endurance limit. These parameters include temperature, prior low-cycle fatigue damage, heat-to-heat variability, thermal aging, weldments, and surface finish. In addition, two other parameters, strain rate and grain size, were found to be significant as the testing program progressed.

This program was conducted as a collaborative effort between Argonne National Laboratory (ANL), Idaho National Engineering Laboratory (INEL), and in part, Risley Nuclear Power Development Laboratories (RNL) in the UK. The objectives of this investigation were set forth in the CRBRP Development Requirements Specification (DRS) 31.1.04.

II. SCOPE

Results are reported for 53 fully reversed, axially loaded high-cycle fatigue tests conducted in (static) laboratory air at temperatures between 482 and 593°C. Included are tests to determine the effects of the parameters described in the preceeding section, as well as the results of two tests conducted at 550°C as part of a US/UK exchange agreement.[1] Design curves based on these high-cycle data and existing low-cycle data at 482 and 593°C are also presented and compared with the current ASME design curves.

III. EXPERIMENTAL PROGRAM

A. Materials and Specimens

The wrought material used in this investigation was obtained from three heats of Type 316 stainless steel. The baseline data were provided from the US reference Heat 8092297 (designated 297). Comparison data were provided from the US Heat 65808 (designated 808) and the UK reference Heat 83. The product forms, grain sizes, and chemical compositions of these heats are given in Table I. For comparison, this table also includes the compositional requirements given by the standard ASTM specification. Table I also lists the composition of the Type 16-8-2 stainless steel weld-filler wire that was used to join 25-mm-thick plates from Heat 297 by the Shield Metal-Arc process.

All of the test specimens were uniform-gauge section type. The wrought specimens machined from the plate material were taken parallel to the rolling direction. All of the wrought specimens were solution annealed (SA) at 1065°C (ANL and INEL) or 1050°C (RNL) for 30 min prior to testing. For the study on thermal aging, specimens were aged in flowing sodium at 593°C for 5000 h prior to testing. Scanning electron micrographs (SEMs) of the specimen surface before and after the 5000-h sodium exposure are shown in Fig. 1.

The weldment specimens were initially oriented transverse to the welding direction and cut from the weldment such that the fusion line was in the center of the gauge length, as specified by DRS 31.1.04. Since the specimens were tested in the as-welded condition, strain was concentrated in the softer parent-metal portion of the gauge section and the specimens failed prematurely. A cross section of the weldment and a hardness profile is shown in Fig. 2. A second group of weldment specimens had the gauge section centered on the centerline of the weld, which meant that they were essentially all weld-metal specimens in the transverse orientation. Testing of the specimens was successful.

Details of the ANL and INEL test specimens are given in Fig. 3. In both specimens, concern over failures outside the extensometer gauge section led to the adoption of a slight taper ($\sim$0.05 mm) from the ends to the center of the uniform-gauge section. A gauge-section surface finish of 0.2 μm (8 μin.) was obtained by mechanical polishing before heat treatment.

Table I. Comparison of Chemistries for Three Heats of Type 316 Stainless Steel and Type 16-8-2 Stainless Steel (E16-8-2-16) Weld Wire

Heat	Product		Grain Size, ASTM (μm)[a]	Chemical Composition (wt %)[b]											
	Form	Size (mm)		C	Mn	P	S	Si	Cr	Ni	Mo	Cu	Ti	Co	N
83	Bar	35	6.0 (49)	0.060	1.82	0.038	0.032	0.46	17.11	12.62	2.56	0.37	0.01	0.24	0.044
297	Plate	16	5.0 (54)	0.068	1.90	0.024	0.020	0.64	17.01	13.36	2.49	0.07	<0.01	0.02	0.034
297	Plate	25	3.2 (103)	0.059	1.84	0.024	0.018	0.58	17.15	13.40	2.34	0.10	<0.01	0.02	0.032
808	Bar	16	4.9 (57)	0.086	1.73	0.010	0.006	0.52	18.16	13.60	2.47	0.078	..	0.074	0.050
ASTM specification[c]	..	..	..	0.08	2.00	0.045	0.030	1.00	16.00-18.00	11.00-14.00	2.00-3.00	..	..	..	0.10
Lot 9A23B mix 8	Weld Wire	3	..	0.07	1.7	0.02	0.02	0.4	15.7	8.5	1.7	0.5	..	..	..

[a]Values for reannealed condition.

[b]Heat 297 (16-mm plate) and 83 data from M. K. Booker, B. C. P. Booker, V. K. Sikka, and C. R. Brinkman, A Comparative Analysis of British and American Tensile and Creep Data for Type 316 Stainless Steel, ORNL/BRP-80/6, Oak Ridge National Laboratory, Oak Ridge, TN (June 1980). Heat 297 (25-mm plate) data from R. J. Beaver and W. R. Martin, Procurement of Type 316 Stainless Steel Reference Heat for LMFBR Research and Development Programs, ORNL/TM-5196, Oak Ridge National Laboratory, Oak Ridge, TN (January 1976). Heat 808 data from J. B. Conway, R. H. Stentz, and J. T. Berling, Fatigue, Tensile, and Relaxation Behavior of Stainless Steels, TID-26135, U.S. Atomic Energy Commission, Washington, D. C. (1975). ASTM specification from "Standard Specification for Heat-Resisting Chromium and Chromium-Nickel Stainless Steel Plate," ASTM Standard A240-80b, 1981 Annual Book of ASTM Standards, Part 4, pp. 191-200. Weld-wire data from Oak Ridge National Laboratory, Mechanical Properties Design Data Program Semiannual Progress Report for Period Ending July 31, 1982, ORNL/MSP/1.3-82/3, pp. 4-25 (October 1982).

[c]Values are permissible maximum or range.

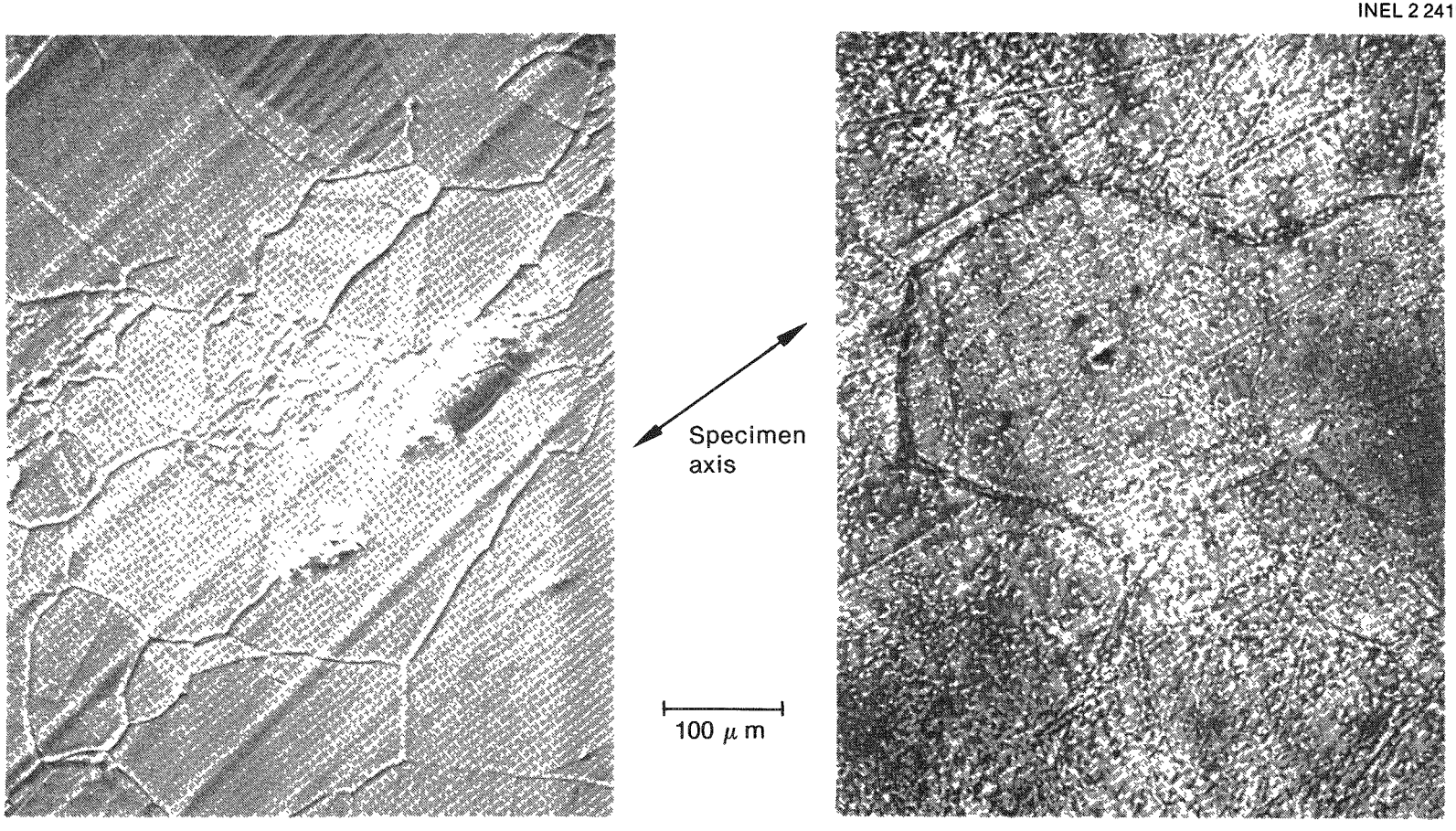

Fig. 1. SEMs of Type 316 SS Fatigue Specimens.

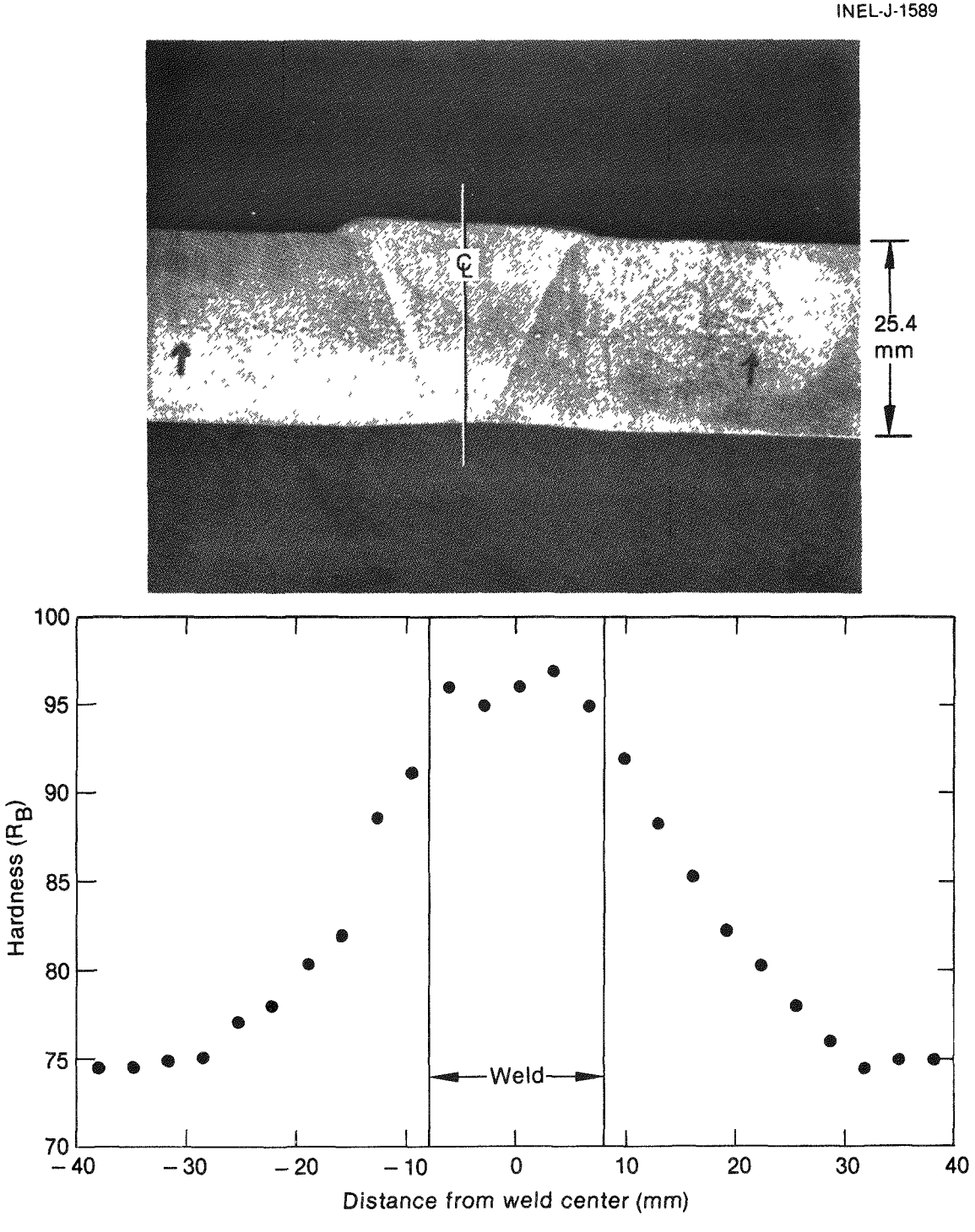

Fig. 2. Hardness Profile of Type 316 SS Weldment.

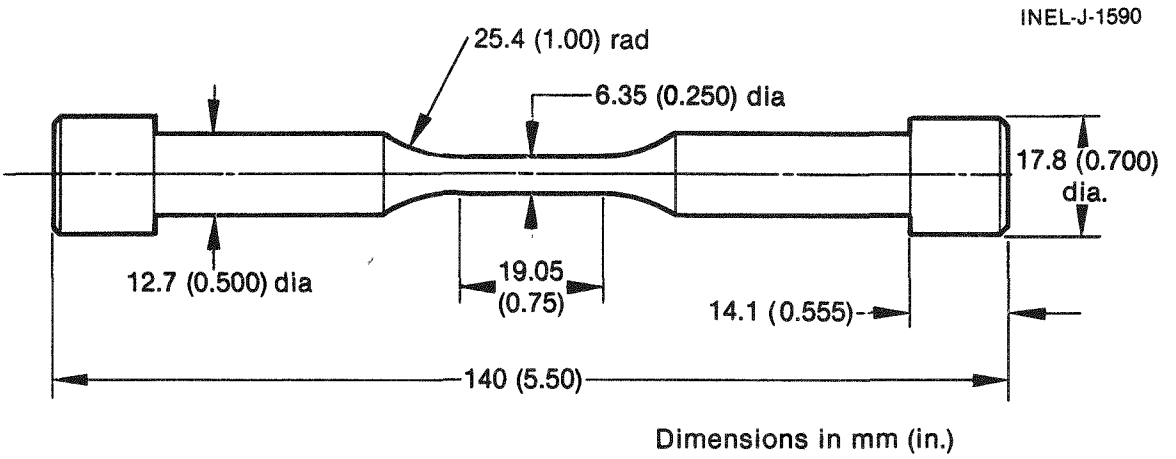

(a)

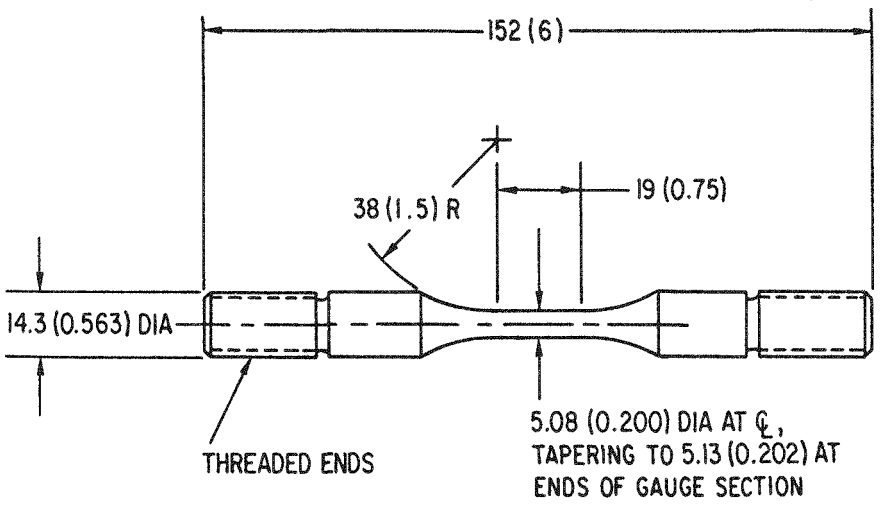

(b)

Fig. 3. Specimen Details for High-cycle Fatigue Tests. (a) ANL specimen. (b) INEL specimen. Dimensions in mm (in.).

B. Apparatus and Test Procedure

All of the tests were conducted on closed-loop hydraulic test systems in (static) laboratory air with cyclic frequencies up to 20 Hz. The control mode for the baseline data was axial strain with a sine-wave loading at a frequency of 1 Hz until the cyclic hardening was completed. Once the cyclic hardening was completed ($\sim 10^6$ cycles), the control mode was switched to axial load at a frequency of 20 Hz. A typical cyclic hardening history is shown in Fig. 4.

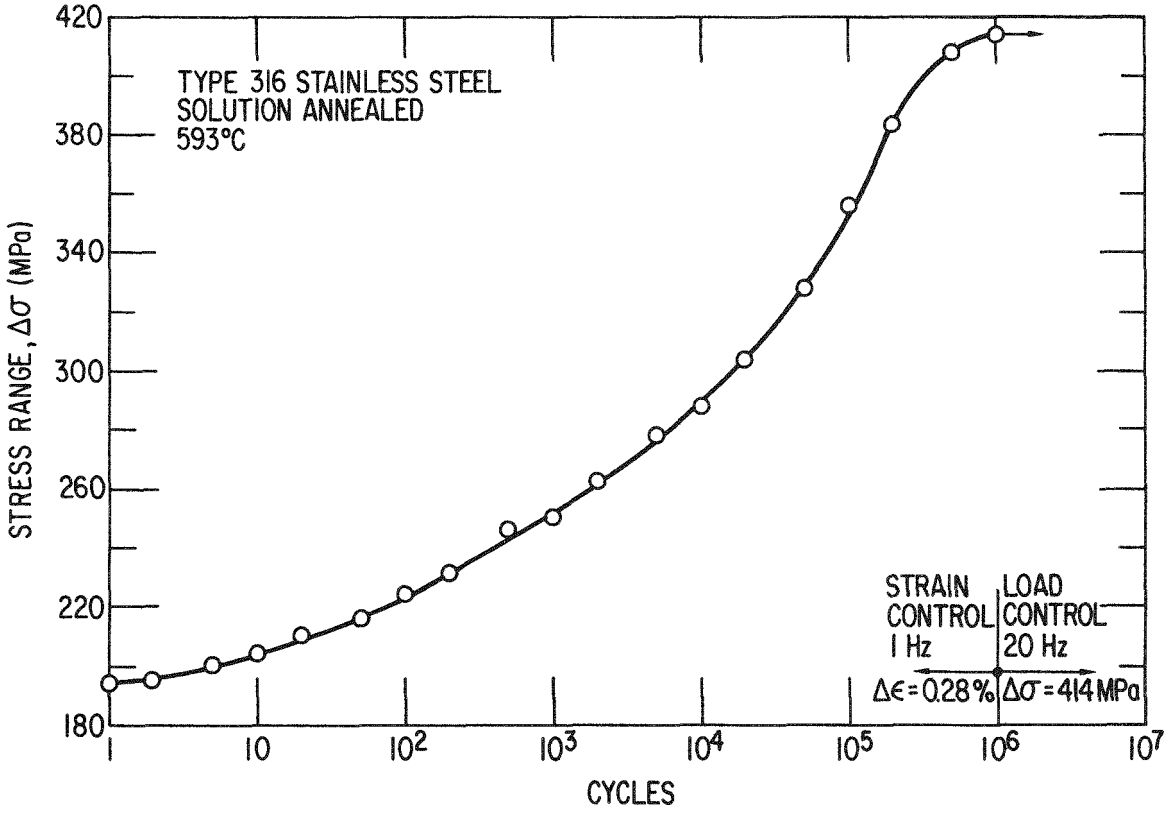

Fig. 4. Example of Cyclic Hardening During Strain-Control Portion of a High-Cycle Fatigue Test (Specimen PU 46).

A number of tests at ANL were conducted using axial stroke control between the shoulders of the specimens (stroke/strain control). This control mode allowed a test frequency of 20 Hz to be obtained much sooner ($\sim 10^4$ cycles) than would be possible in axial strain control. Thus, the total test duration was shortened considerably. The cyclic strain ranges were maintained by periodically reducing the test frequency and monitoring the signal from an axial extensometer. The test setup is shown schematically in Fig. 5 and described in detail in Ref. 2. Although this testing procedure was successful, it was subsequently abandoned because of the strong effect of strain rate (frequency) on the high-cycle fatigue behavior of this steel (this will be discussed in the next section). In order to investigate systematically the effect of test frequency on fatigue life, a number of tests were conducted in axial strain control to failure.

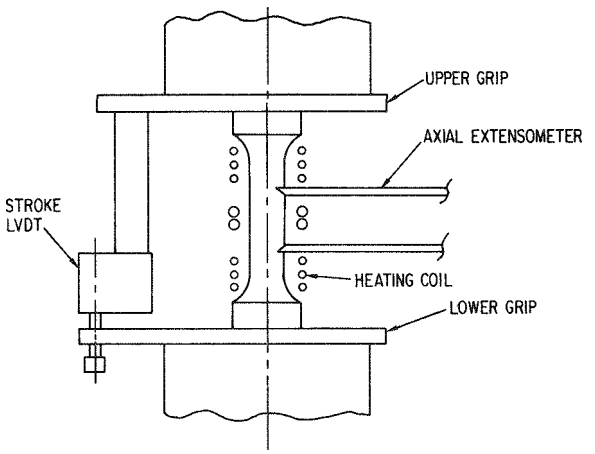

Fig. 5

Schematic Illustration of the High-Cycle Fatigue Test Setup.

As shown in Fig. 5, the specimens were heated by an induction coil operating at 455 kHz. The coil was designed to provide a relatively flat temperature profile (±3°C) over the critical gauge section. This heating arrangement is typical for all the tests conducted at ANL and INEL. At RNL, specimen heating was by an electrical-resistance furnace.

IV. RESULTS AND DISCUSSION

A. General Results

All of the high-cycle fatigue test data generated in this investigation are given in Table II. Included are 26 tests conducted at ANL, 25 tests at INEL, and 2 tests at RNL. This table also notes the purpose for which each of these tests were conducted. A summary of the tests by purpose and contributing laboratory is given in Table III.

B. Baseline Data

As described previously, the baseline data were generated at 593°C under axial strain control at 1 Hz until the cyclic hardening saturated, then the test was switched to load control at 20 Hz. The majority of tests used sine-wave loading although a number of tests were conducted with a triangular waveform as noted in Table II. This data base was combined with existing data at 593°C[3] to obtain the strain-life curves shown in Fig. 6. As indicated, there is a separate curve for each of the material grain sizes associated with the 16- and 25-mm-thick plates used in this study. The strong effect of grain size on the high-cycle fatigue behavior shown in this figure was not fully appreciated until the testing program was nearly completed. Thus the bulk of the data generated at ANL came from 16-mm plate (ASTM 5.0 grain size), while most of the data generated at INEL came

from 25-mm plate (ASTM 3.2 grain size). The strain-life relations shown in Fig. 6 are the result of a non-linear regression analysis on the data shown and are discussed in Appendix A. Using these relations, the 10^8-cycle endurance strain limits were determined to be 0.271% for data with a grain size of ASTM 5.0 and 0.242% for a grain size of ASTM 3.2.

The strong dependence of high-cycle fatigue behavior on grain size for this steel must be considered in design. Components fabricated from thick ($\geq$100 mm) plates can be expected to have a grain size of about ASTM 3 (110 μm) with some areas even coarser.[4] This coarse grain size and subsequent low value of the 10^8-cycle design strain range can have a significant effect on the design of the above core components of CRBRP. Thus it may be necessary to avoid the use of thick-section plates for this application. The determination of the 10^8-cycle endurance strain limit for other grain sizes is beyond the scope of the present study; however, it is part of the ongoing program at ANL.[5]

The fatigue curves shown in Fig. 6 were reduced by a factor of two for strain range or twenty for fatigue life to obtain fatigue design curves. The resulting curves were refit to relations similar to those shown in Fig. 6 and are plotted in Fig. 7 (the dashed portions of these curves represent extrapolation beyond the data base). For comparison, the current ASME code case N-47 design curve is also given in this figure.[6] The results show that even for very large-grained steel the ASME curve is extremely conservative. Direct numerical comparisons of allowable strain ranges for the present curves and the ASME curve are given in Table IV. These results indicate that for a given high-cycle strain range, the present curves give improvements in fatigue life in excess of three orders of magnitude over the ASME curve.

C. Test Method Development/Strain Rate Effects

In the course of the present study, significant differences in fatigue lives were observed between the tests conducted at ANL and at INEL. As discussed in the preceeding section, this was in part due to a strong grain size dependence in this steel. Differences in test procedures also contributed significantly. The data generated at INEL were generally obtained at a strain-controlled test frequency of 1 Hz while the early ANL data were obtained in stroke/strain control at frequencies of from 0.2 to 20 Hz.[7] This high-frequency testing on material that was not fully cyclically hardened resulted in longer fatigue lives than would otherwise be obtained. Unfortunately, this was not readily apparent because several of the INEL tests employed a sine-wave loading which obscured the calculation of a strain rate and the ANL tests employed a range of test frequencies between 0.2 and 20 Hz which also made the calculation of an "average" strain rate difficult. Once this effect was discovered, however, a number of tests were performed at both ANL[8] and INEL[9]. The results of these tests are listed in Table II and shown in Fig. 8. In all cases, the data shown in this figure were obtained from constant axial strain rate tests at the cyclic frequencies indicated. The dashed lines in this figure are intended only to show the envelope of the data, and since the ANL and INEL data were obtained from specimens with different grain sizes, no

Table II. Results[a] of High-cycle Fatigue Tests on Type 316 Stainless Steel

Lab[b]	Specimen Number (Test Number)	Plate Thickness (mm)[c]	Wave Form, Strain and Load Control[d]	Range (%) $\Delta\varepsilon_t$	Range (%) $\Delta\varepsilon_p$[e]	Stress Range (MPa)	Strain Control Cycles	Strain Control Frequency (Hz)	Strain Rate, s^{-1}	Load Control Cycles	Load Control Frequency (Hz)	Total Fatigue Life N_f	Total Fatigue Life t_f (h)	Purpose of Test
						Test Temperature = 482°C								
INEL	DR-34	25	S	0.26	0.001	383	1.000×10^{6}	1	..	1.457×10^{8}	20	1.467×10^{8}	2301	Temp. Effects
INEL	DR-7	25	S	0.25	0.006	405	1.062×10^{6}	1	..	1.091×10^{8}	20	1.102×10^{8}	1810	Temp. Effects
						Test Temperature = 550°C								
ANL	PU2A[f] (288)	16	T	0.35	0.000	544	5.286×10^{6}	1	7.0×10^{-3}	..		5.286×10^{6}	1473	US/UK Exch.
ANL	83-5[f] (319)	35[g]	T	0.35	0.013	519	1.529×10^{7}	1	7.0×10^{-3}	3.540×10^{5}	20	1.564×10^{7}	4252	US/UK Exch.
						Test Temperature = 593°C								
ANL	PU17 (290)	16	T	0.33	0.024	462	9.800×10^{5}	1	6.6×10^{-3}	..	..	9.800×10^{5}	274	Baseline Data
ANL	PU42 (303)	16	T	0.33	0.020	467	3.568×10^{6}	1	6.6×10^{-3}	..	..	3.568×10^{6}	975	"
ANL	PU24 (311)	16	T	0.33	0.023	460	5.086×10^{6}	1	6.6×10^{-3}	..	..	5.086×10^{6}	1412	"
ANL	PU19 (292)	16	T	0.33	0.014	473	2.735×10^{6}	5	3.3×10^{-2}	..	..	2.735×10^{6}	155	Strain Rate Effects
ANL	PU20A (296)	16	T	0.33	0.017	468	6.163×10^{6}	5	3.3×10^{-2}	..	..	6.163×10^{6}	342	"
ANL	PU16 (294)	16	T	0.33	0.015	472	1.209×10^{7}	10	6.6×10^{-2}	..	..	1.209×10^{7}	349	"
ANL	PU41 (299)	16	T	0.33	0.015	471	1.392×10^{7}	10	6.6×10^{-2}	..	..	1.392×10^{7}	387	"
ANL	PU27 (316)	16	T	0.33[h]	0.013	474	2.029×10^{7}	20	1.3×10^{-1}[i]	..	..	2.029×10^{7}	293	"
ANL	PU12 (268)	16	T	0.33[h]	0.036	438	7.870×10^{5}	0.2-20	1.1×10^{-3}[i]	..	..	7.870×10^{5}	257	Baseline Data
ANL	PU13 (272)	16	T	0.33[h]	0.027	454	1.219×10^{6}	0.2-20	4.2×10^{-2}[i]	..	..	1.219×10^{6}	144	Test Meth. De
ANL	PU9 (287)	16	T	0.30[h]	0.007	439	1.112×10^{7}	0.5-5	1.4×10^{-2}[i]	..	..	1.112×10^{7}	648	"
ANL	PU1 (275)	16	T	0.30[h]	0.000	449	2.999×10^{7}	0.2-20	4.8×10^{-2}[i]	..	..	2.999×10^{7}	455	"
ANL	PU3 (280)	16	T	0.30[h]	0.011	432	3.123×10^{7}	0.2-20	6.1×10^{-2}	..	..	3.123×10^{7}	464	"
ANL	PU8 (284)	16[j]	T	0.30	0.017	423	1.217×10^{6}	0.67	4.0×10^{-3}	5.391×10^{6}	20	6.608×10^{6}	577	Baseline Data
ANL	PU30 (326)	16[j]	S	0.29	0.013	415	1.199×10^{6}	1	..	1.868×10^{7}	20	3.067×10^{7}	359	"
ANL	PU48 (312)	16	S	0.28	0.003	415	1.030×10^{6}	1	..	1.384×10^{7}	20	1.487×10^{7}	479	"
ANL	PU46 (309)	16	S	0.28	0.004	414	1.033×10^{6}	1	..	3.432×10^{7}	20	3.535×10^{7}	764	"
ANL	PU26 (314)	16	S	0.28[h]	0.003	415	1.034×10^{6}	1	..[i]	6.728×10^{7}	20	6.831×10^{7}	1223	"
ANL	PU4 (278)	16	T	0.28[h]	0.000	419	1.658×10^{8}	0.2-20	3.9×10^{-2}[i]	..	..	1.658×10^{8}	2417	Test Meth. Da
ANL	PU5 (286)	16	T	0.28[h]	0.000	419	2.010×10^{8}	0.2-20	2.6×10^{-2}	..	..	2.010×10^{8}	2926	"
ANL	808-1A (329)[k]	16[g]	S	0.27	0.000	417	1.202×10^{6}	1	..	8.467×10^{6}	20	9.669×10^{6}	452	Heat-to-Heat Effects
ANL	83-4 (328)[f,l]	35[g]	S	0.27	0.013	384	1.617×10^{6}	1	..	9.848×10^{7}	20	$>1.001\times10^{8}$	>1818	"
ANL	PU25 (327)[l]	16	S	0.27	0.009	390	1.036×10^{6}	1	..	9.906×10^{7}	20	$>1.001\times10^{8}$	>1663	Prior Plastic Def.
ANL	PU28 (320)	16	S	0.26	0.003	385	1.011×10^{6}	1	..	1.020×10^{8}	20	$>1.030\times10^{8}$	>1700	Baseline Data
INEL	DR-6	25	T	0.35	0.043	480	2.434×10^{5}	0.57	4.0×10^{-3}	..	..	2.434×10^{5}	38	"
INEL	DR-39	25	S	0.33	0.047	428	2.388×10^{5}	1	..	..	..	2.388×10^{5}	66	"
INEL	DR-31	25	T	0.33	0.027	409	4.265×10^{5}	1	6.6×10^{-3}	..	..	4.265×10^{5}	118	"
INEL	DR-38	25	T	0.33	0.008	422	1.155×10^{6}	1	6.6×10^{-3}	..	..	1.155×10^{6}	321	"
INEL	DR-42	25	T	0.33	..	..	6.934×10^{6}	5	3.3×10^{-2}	..	..	6.934×10^{6}	1926	Strain Rate Effects

Test Temperature = 593°C

INEL	DR-9	25	T	0.32	0.023	449	9.109×10^{5}	0.63	4.0×10^{-3}	..	..	9.109×10^{5}	159	Baseline Data
INEL	DR-52	25	T	0.31	..	419	6.990×10^{5}	1	6.2×10^{-3}	..	..	6.990×10^{5}	194	"
INEL	DR-27	25	S	0.29	0.026	426	1.214×10^{6}	1	..	4.616×10^{5}	20	1.675×10^{7}	344	"
INEL	DRA-2	16	S	0.29	0.008	432	1.024×10^{6}	1	..	1.790×10^{6}	20	1.893×10^{7}	533	"
INEL	DR-53	25	S	0.28	0.008	399	1.204×10^{6}	1	..	1.630×10^{6}	20	2.834×10^{6}	357	"
INEL	DR-55	25	S	0.28	0.006	418	1.196×10^{6}	1	..	6.096×10^{6}	20	7.292×10^{6}	417	"
INEL	DR-22	25	S	0.28	0.013	411	1.033×10^{6}	1	..	7.717×10^{6}	20	8.750×10^{6}	394	"
INEL	DRA-1	16	S	0.28	0.002	419	1.104×10^{6}	1	..	1.171×10^{7}	20	1.281×10^{7}	469	"
INEL	DR-33	25	T	0.28	0.007	404	1.001×10^{6}	1	5.6×10^{-3}	1.832×10^{7}	20	1.932×10^{7}	532	"
INEL	DR-56	25	T	0.27	0.001	398	1.000×10^{6}	1	5.4×10^{-3}	1.588×10^{7}	20	1.688×10^{7}	498	"
INEL	DR-24	25	S	0.26	0.014	381	8.478×10^{5}	1	..	9.928×10^{6}	20	1.078×10^{7}	373	"
INEL	DR-29	25	S	0.25	0.007	378	1.095×10^{6}	1	..	3.010×10^{7}	20	3.119×10^{7}	722	"
INEL	DR-35	25	S	0.24	0.006	371	1.108×10^{6}	1	..	6.074×10^{7}	20	6.201×10^{8}	1151	"
INEL	DR-13	25	S	0.24	0.007	387	1.202×10^{6}	1	..	1.337×10^{8}	20	1.349×10^{8}	2191	"
INEL	DR-30[m]	25	S	0.24	0.017	331	1.325×10^{7}	1-11[n]	..	..	..	1.325×10^{7}	1240	Effect of Aging
INEL	DR-19[m]	25	S	0.24	0.024	315	1.051×10^{6}	1	..	2.150×10^{7}	20	2.256×10^{7}	591	"
INEL	DRW-7[o]	25	S	0.24	0.005	273	1.016×10^{6}	1	..	1.419×10^{7}	20	1.520×10^{7}	479	Weldment Test
INEL	DRW-9[o]	25	S	0.24	0.012	278	1.000×10^{6}	1	..	1.920×10^{7}	20	2.020×10^{7}	544	"
RNL[p]	KD1 (S3/15)	25[q]	T	0.35	..	475	2.250×10^{5}	1	7.0×10^{-3}	..	..	2.250×10^{5}	62	US/UK Exch. &
RNL[p]	KD2 (S3/16)	25[q]	T	0.31	..	448	5.510×10^{6}	1	6.2×10^{-3}	..	..	5.510×10^{6}	1531	Baseline Data

[a] Fully reversed axial loading, strain ratio R = -1, tested in air, $\Delta\varepsilon_t$ = total strain range, $\Delta\varepsilon_p$ = plastic strain range, N_f = cycles to failure, and t_f = time to failure.

[b] ANL = Argonne National Laboratory, INEL = Idaho National Engineering Laboratory, RNL = Risley Nuclear Power Development Laboratories (UK).

[c] 25-mm-thick plate has a grain size of ASTM 3.2 (103 μm), 16-mm-thick plate has a grain size of ASTM 5.0 (54 μm), 35-mm-dia. bar has a grain size of ASTM 6.0 (39 μm), 16-mm-dia. bar has a grain size of ASTM 4.9 (57 μm).

[d] S = sine, T = triangular.

[e] These values were taken at $N_f/2$ for tests that failed in strain control. If the test was switched to load control, then this value is that at the end of the strain control portion.

[f] UK Heat 83, used for heat-to-heat variability study.

[g] Round bar.

[h] These tests were conducted under stroke/strain control (see text, III.B).

[i] Effective value during cyclic hardening (see text).

[j] Annealed 72 h at 1065°C, grain size = ASTM 2.7 (123 μm).

[k] Heat 808, used for heat-to-heat variability study.

[l] Used for prior plastic deformation study, prestrained 1000 cycles at 0.5%.

[m] Aged in flowing sodium for 5000 h at 593°C prior to testing.

[n] Cycled at 1 Hz for first 3.584×10^{6} cycles, then 11 Hz to failure.

[o] Transverse, as-welded, all weld-metal specimen.

[p] From D. S. Wood at the US/UK Exchange Meeting on the Fatigue Behavior of Type 316 stainless steel at ANL on June 17, 1981.

[q] Heat 297 grain size ASTM 3.2 (103 μm).

Table III. Type 316 Stainless Steel High-Cycle Fatigue Data Generated in the Present Investigation, Summarized by Contributing Laboratory

Purpose of Test	Number of Tests at Laboratory[a]			
	ANL	INEL	RNL	Total
Baseline Data at 593°C	10	18	2	30
Test Method Development	6	0	0	6
Strain Rate Effects	5	1	0	6
Temperature Effects at 482°C	0	2	0	2
Prior Low-Cycle Fatigue Damage	1	0	0	1
Heat-to-Heat Variability	2	0	0	2
Thermal Aging Effects	0	2	0	2
Weldment Tests	0	2	0	2
Surface Finish Effects	0	0	..[b]	..
US/UK Data at 550°C	2	0	0	2
Total	26	25	2	53

[a]ANL = Argonne National Laboratory, INEL = Idaho National Engineering Laboratory, and RNL = Risley Nuclear Power Development Laboratories (UK).

[b]As of this printing, the exchange of these data has not been concluded.

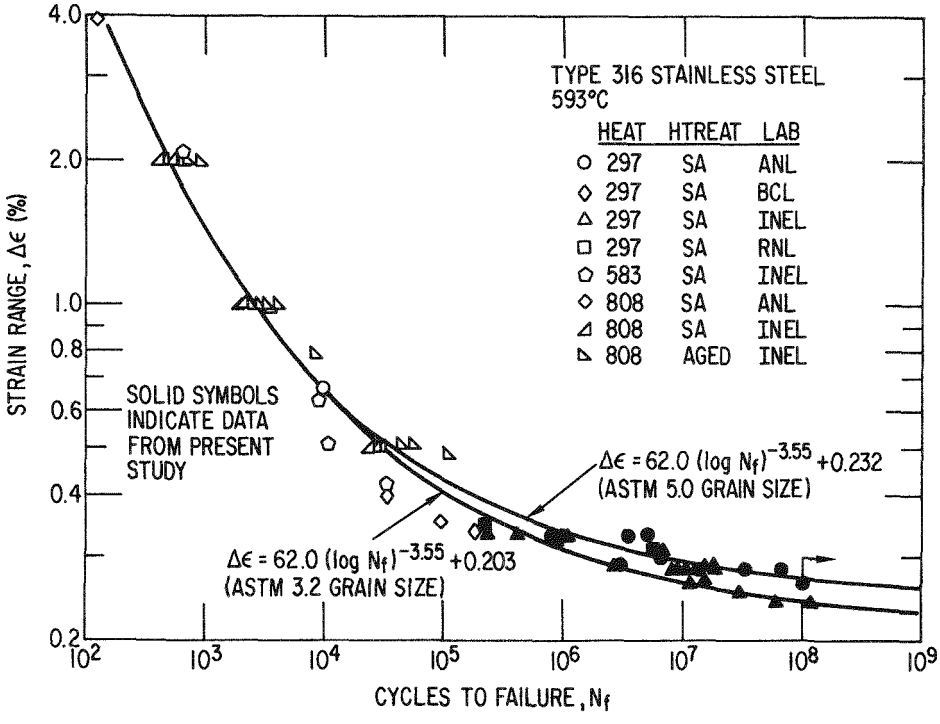

Fig. 6. Type 316 Stainless Steel Fatigue Data at 593°C.

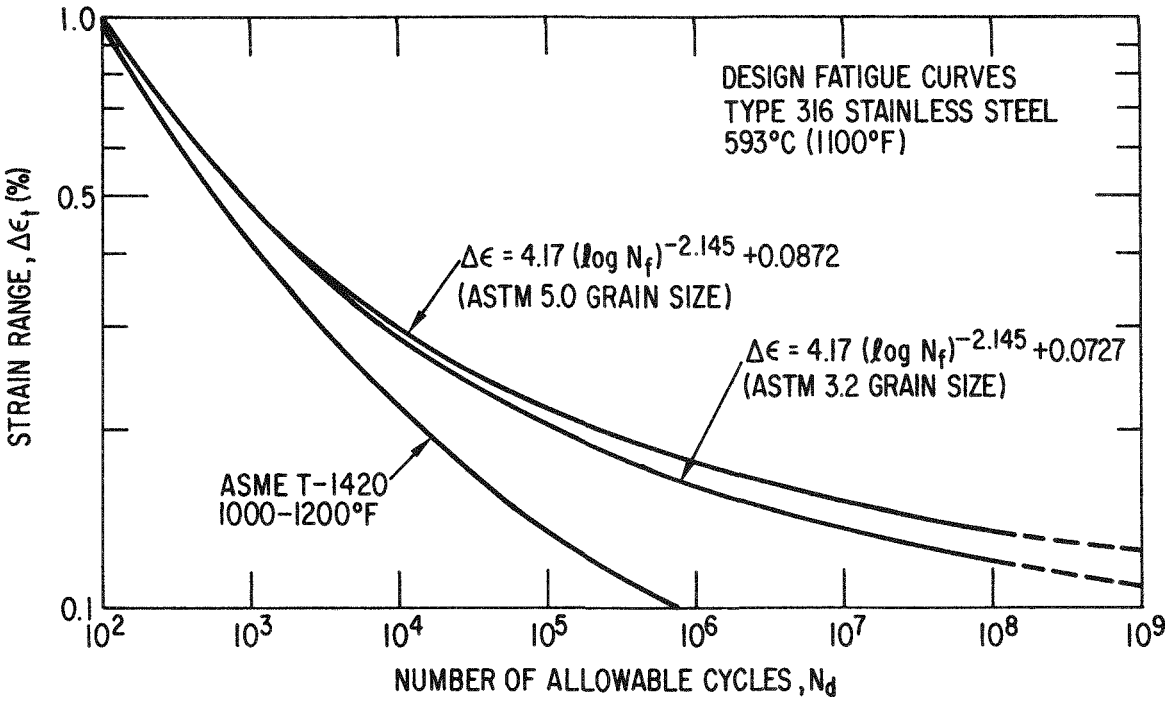

Fig. 7. Fatigue Design Curves for Type 316 Stainless Steel at 593°C (1100°F).

Table IV. Design Fatigue Strain Range, $\Delta\varepsilon_t$(%), for Type 316 Stainless Steel at 593°C (1100°F)

Number of Cycles, N_d	Strain Range, $\Delta\varepsilon_t$(%)		
		Present Study	
	ASME T-1420	ASTM 3.2 Grain Size	ASTM 5.0 Grain Size
10^2	0.974	1.02	1.03
10^3	0.424	0.468	0.482
10^4	0.221	0.286	0.300
10^5	0.136	0.205	0.219
10^6	0.096	0.162	0.177
10^7	..	0.137	0.151
10^8	..	0.121	0.135
10^9	..	0.110[a]	0.125[a]

[a]Extrapolated value.

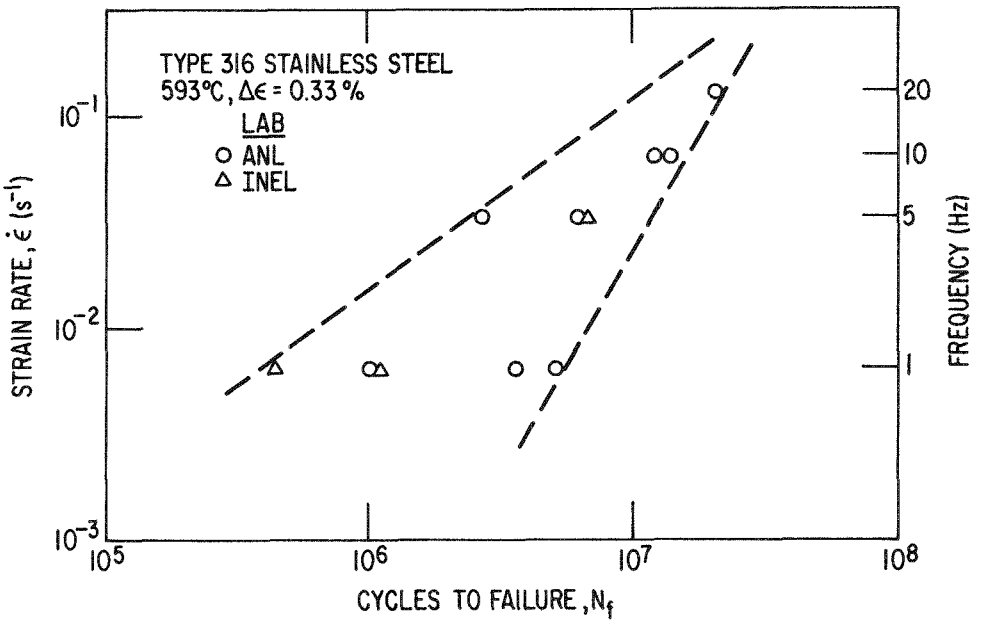

Fig. 8

The Effect of Strain Rate on the High-Cycle Fatigue Behavior of Type 316 Stainless Steel.

attempt was made to combine the data for analysis. Nevertheless, the trend of these data indicates that in the high-cycle fatigue regime, an increase in cyclic frequency from 1 to 20 Hz during the cyclic hardening phase will increase the fatigue life by about a factor of 7. This conclusion is also supported by the ANL data at test frequencies between 0.2 and 20 Hz. If an "effective" strain rate based on the percentage of total cyclic hardening at a given frequency is defined, then the trend for data at a strain range of 0.30% produce virtually identical results to those shown in Fig. 8. In comparison, low-cycle fatigue data ($\Delta\varepsilon \sim 0.5\%$) on Type 304 stainless steel (which is similar to Type 316 in low-cycle fatigue behavior) give only a factor of 2 increase in life for a factor of 20 increase in strain rate.[10]

An estimate of the 10^8-cycle endurance strain range for the data in Table II generated at 5, 10, and 20 Hz was obtained by drawing a new curve through the data parallel to the appropriate curve in Fig. 6. These estimates are tabulated in Table V.

D. Temperature Effects

One of the DBS requirements was to investigate the effect of temperature on the 10^8-cycle endurance strain range determined at 593°C. These tests were intended to show that a decrease in temperature from 593°C (1100°F) to 482°C (900°F) does not result in a decrease in the 10^8-cycle endurance strain limit. To accomplish this, two tests were conducted at 482°C with a strain range of 0.26 and 0.25%. Since these specimens (DR-34 and DR-7) had a grain size of ASTM 3.2, the corresponding endurance strain range was 0.24%. As indicated in Table II, both specimens failed beyond the 10^8-cycle limit and thus no further testing at this temperature was required.

Table V. 10^8-Cycle Strain Ranges for Type 316 Stainless Steel at 593°C

Parameter	Grain Size, ASTM	10^8-Cycle Strain Range (%)
Baseline Data	3.2	0.242
Baseline Data	5.0	0.271
Test Frequency of 5 Hz	5.0	0.29[a]
Test Frequency of 10 Hz	5.0	0.31[a]
Test Frequency of 20 Hz	5.0	0.32[a]
Data at 482°C	3.2	0.255
Prior Low-Cycle Fatigue Damage	5.0	>0.27[b]
Heat 83	6.0	>0.27[b]
Heat 808	4.9	0.25[a]
Pre-aged in Sodium	3.2	0.22[a]
Weldments	..	0.22[a]

[a]Estimated.

[b]Test terminated before failure at this strain range.

As with the 593°C data, these data were combined with existing data to provide a strain-life curve. The curve based on the actual data for a temperature of 482°C is given in Fig. 9, and the corresponding design curve in Fig. 10. These curves were derived using the same procedures used for the 593°C data. A comparison of the design curves at 482 and 593°C is given in Fig. 11. The difference in these curves is not large, and is considerably less than the difference between both ASME curves. At 482°C, the calculated 10^8-cycle design strain range is 0.127%, which is not much higher than the 593°C value of 0.121%.

Two tests listed in Table II (specimens PU2A and 83-5), but not a part of the DRS, were conducted at 550°C (1022°F) as part of the US/UK collaborative program. The result of the test on the specimen (PU2A) from Heat 297 is unusual because the fatigue life is considerably longer than the results at 482°C and 593°C would predict. The difference in fatigue lives between the specimens from Heats 297 and 83 at 550°C is probably due to the finer grain size for Heat 83 material (see Table I).

E. Prior Low-Cycle Fatigue Damage

In order to assess the effect of occasional overloads on the baseline 10^8-cycle endurance strain range, one specimen (PU25) was prestrained for 1000 cycles at a strain range of 0.5%. This was followed by routine high-cycle fatigue testing at a strain range of 0.27% (the endurance strain limit for fine-grained material). The test was terminated after this specimen completed 10^8 cycles without failure. A plot of the cyclic hardening behavior for this specimen is given in Fig. 12. The results of this test imply that occasional overloads not exceeding a strain range of 0.5% will not cause enough damage to reduce the high-cycle fatigue

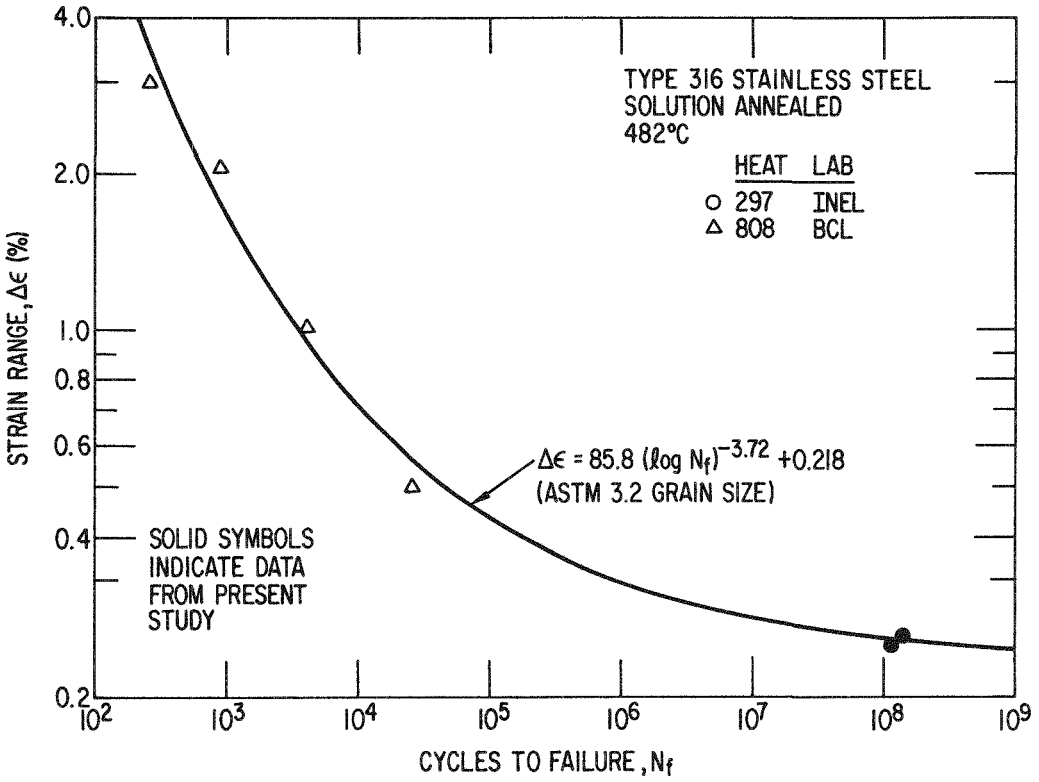

Fig. 9. Type 316 Stainless Steel Fatigue Data at 482°C.

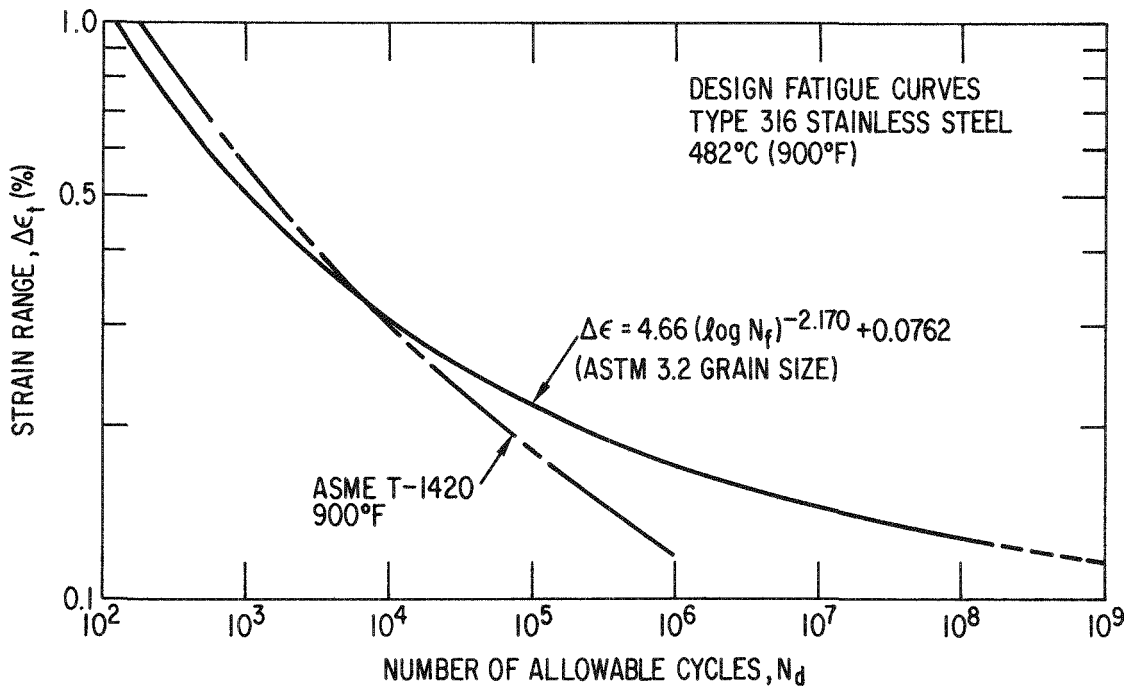

Fig. 10. Fatigue Design Curves for Type 316 Stainless Steel at 482°C (900°F).

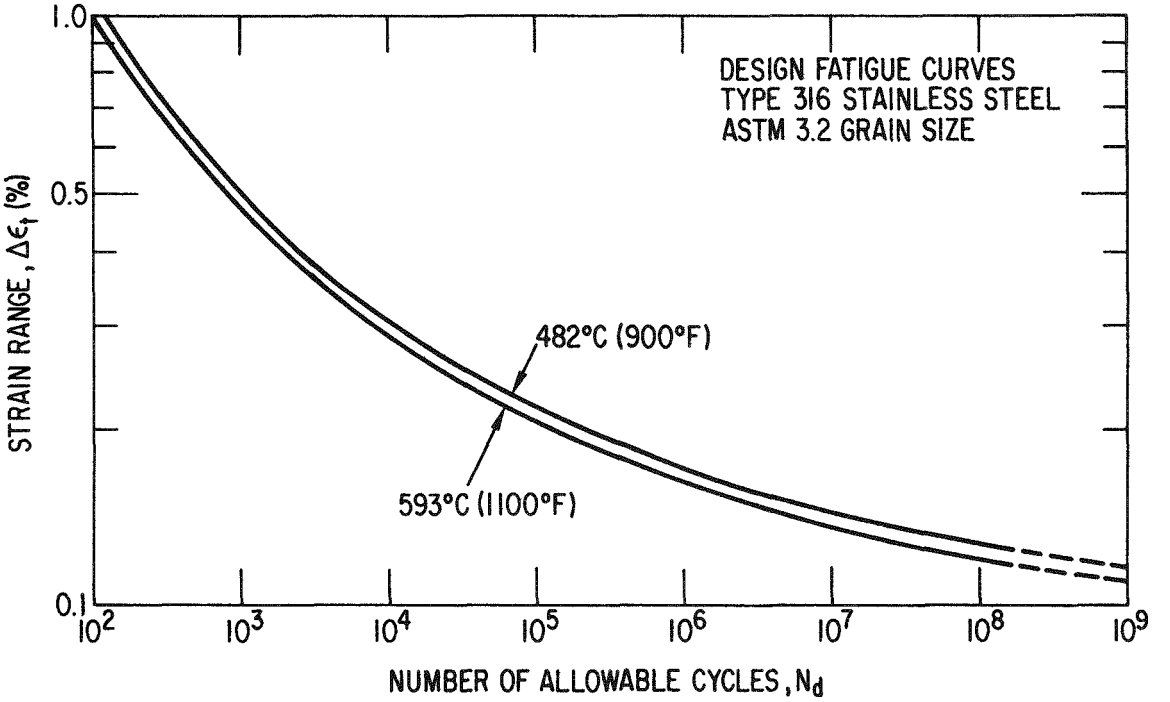

Fig. 11. Comparison of Fatigue Design Curves for Type 316 Stainless Steel.

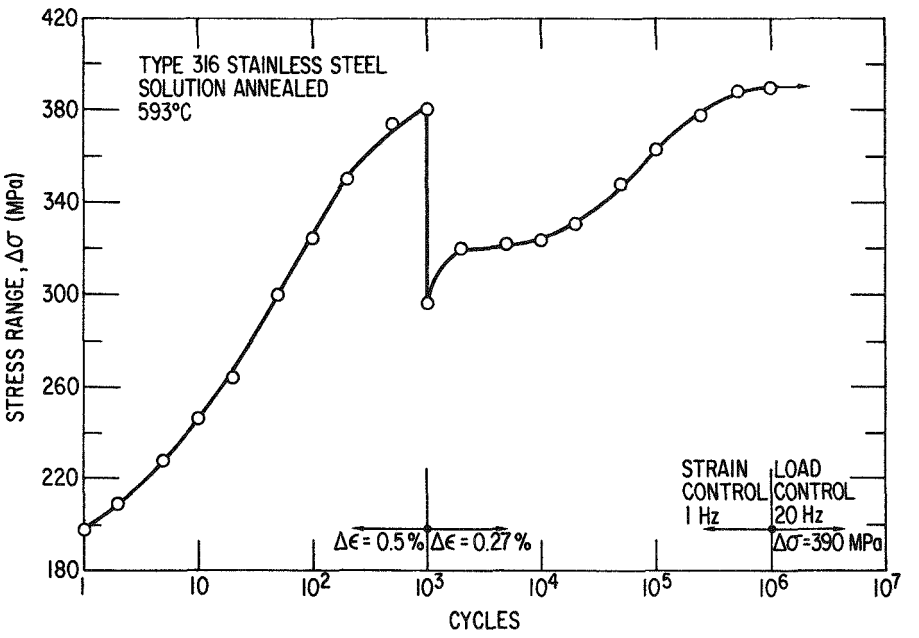

Fig. 12. Cyclic Hardening During Strain-Control Portion of a Test for the Effect of Prior Low-Cycle Fatigue Damage (Specimen PU 25).

life of a structural component. This was also demonstrated in earlier tests at ANL[8] where prior straining at 0.5% for up to 5000 cycles produced no premature failures in high-cycle tests at a strain range of 0.33%.

F. Heat-to-Heat Variability

The heat-to-heat variation of the 10^8-cycle endurance strain limit was investigated. Two tests using specimens from Heat 808 (specimen 808-1A) and the UK reference Heat 83 (specimen 83-4) were conducted at a strain range of 0.27% and, as indicated in Table II, the fatigue life for the specimen from Heat 808 was $\sim 9.7 \times 10^6$ cycles whereas the specimen from heat 83 survived 10^8 cycles without failure. In the latter case, the test was terminated as allowed by the DRS. In the case of the specimen from Heat 808, the grain size was similar to that of Heat 297 (ASTM 5.0), although the original product form was bar stock rather than plate. Nevertheless, the fatigue life for the Heat 808 specimen was closer to the results obtained on the large-grained specimens from Heat 297 (ASTM 3.2). The estimated 10^8-cycle endurance strain range for Heat 808 is given in Table V. The large difference in fatigue lives from these tests is contrary to the results obtained in a low-cycle ($\Delta\varepsilon \geq 0.6\%$) fatigue study on the same heats.[11] In the low-cycle study, no significant difference in fatigue life was observed for continuous cycling tests. However, for tests with a hold time at the peak tensile strain (creep fatigue), significant differences in life were obtained, with specimens from Heat 83 having the best performance followed by Heat 297 and then 808. Since the failure mechanisms for continuous-cycling and creep-fatigue tests are basically different,* the correlation between high-cycle and creep fatigue may be coincidental. In the low-cycle creep-fatigue study, it was found that the chromium and nickel equivalents for these three heats decreased with increasing creep-fatigue resistance. This may affect the grain-boundary precipitates which, in turn, can affect the damage. In the present study, however, there does not seem to be any obvious mechanistic explanation for the results obtained.

G. Thermal Aging Effects

In two tests to study the effect of pretest thermal aging, both specimens (DR-30 and DR-19) had fatigue lives that were almost an order of magnitude less than 10^8 cycles. Thus the endurance strain range for aged specimens is less than the unaged endurance strain range of 0.24%. An estimate of 0.22% for this strain range was obtained by the same method used for the high-frequency test data in section IV.

The reduction in endurance strain of the sodium-aged specimens is believed to be due to the aging rather than to any surface modification. Crack initiation on one of the sodium aged specimens was approximately 1.5 mm below the surface. The aged material did not cyclically harden to the same degree as the unaged material and a small inelastic strain component

---

*Transgranular failure after surface crack initiation for continuous-cycling tests versus intergranular failure after grain boundary damage for creep-fatigue tests.

persisted throughout the test. One of these specimens (DR-30) was tested in strain control for the entire duration of the test: 1 Hz for the first 3.6×10^6 cycles and then 11 Hz strain control until failure at 13.2×10^6 cycles.

H. Weldment Tests

As indicated in Section III, the weld-metal specimens (DRW-7 and DRW-9) were machined transverse to the welding direction and tested in the as-welded condition. These specimens were tested at a strain range of 0.24% and had fatigue lives virtually identical to the thermally aged wrought specimens. Thus the estimated 10^8-cycle endurance strain range is also 0.22%.

As in the heat-to-heat variability study, the results obtained in the present study are contrary to the results of a similar low-cycle fatigue study.[12] In the low-cycle fatigue tests ($\Delta\varepsilon \geq 0.5\%$), the weld-metal specimens had lives that were somewhat longer than for the wrought material. These results indicate that there is some strain range between 0.5 and 0.24% where a crossover between wrought and weld-metal fatigue resistance exists. To investigate this effect is beyond the scope of the present study, but further tests on Type 16-8-2 stainless steel weldments are planned.[13]

I. Surface Finish Effects

These tests are being carried out in the UK as part of the US/UK collaborative program. As of this printing, the exchange of these data has not been concluded. When obtained, they will be published separately.

V. SUMMARY AND CONCLUSIONS

The objective of this investigation was twofold: First, to determine the endurance strain limit in Type 316 stainless steel for a cyclic life of 10^8 cycles at 593°C. Second, to investigate the effects of a number of key parameters on this endurance strain limit. These results are summarized in Table V, which lists the 10^8-cycle calculated or estimated strain ranges for the baseline data and the parameters investigated. Based on these results, the following conclusions appear justified:

(a) The 10^8-cycle endurance strain range is very sensitive to the material grain size. Fine-grained material has a higher 10^8-cycle strain range than coarse-grained material. In terms of fatigue life in the strain range of interest, fine-grained materials can have lives more than an order of magnitude greater than coarse-grained material.

(b) This endurance strain range is also strongly affected by the frequency of loading during the cyclic hardening phase. High strain rates result in high endurance strain ranges. A change in loading rate from 1 to 20 Hz can increase the fatigue life by a factor of about 7.

(c) As the temperature is decreased, the endurance strain range increases. Between 482 and 593°C the endurance strain range increases by about 5%.

(d) Limited amounts of prior low-cycle fatigue damage at a strain range of 0.5% do not affect the endurance strain range.

(e) Differences in heat chemistry also affect the endurance strain limit. At a given strain range, the fatigue lives for different heats can differ by an order of magnitude.

(f) Pre-test thermal aging in sodium lowers the endurance strain range by about 8%.

(g) Use of as-welded all weld-metal specimens also lowers the endurance strain range by about 8%.

(h) The effect of surface finish on the endurance strain range is presently unknown.

ACKNOWLEDGMENTS

The authors are grateful for the support and encouragement given by Dr. J. A. Horak of the Oak Ridge National Laboratory Materials and Structures Technology Management Center (ORNL/MSTMC).

REFERENCES

1. C. R. Brinkman, Report of USDOE/UKAEA Exchange Meeting on the Mechanical Properties of Structural Materials for Fast Breeder Reactor Service, Oak Ridge National Laboratory, ORNL/TM-7601 (October 1980).

2. S. Majumdar, D. T. Raske, and W. F. Burke, "A Procedure for Strain-Controlled High-Cycle Fatigue Testing at Elevated Temperatures," J. Test. Eval. 9(1), 35-38 (January 1981).

3. D. R. Diercks, A Compilation of United States and British Elevated-Temperature, Strain-Controlled Fatigue Data on Type 316 Stainless Steel, Argonne National Laboratory, Argonne National Laboratory Report ANL/MSD-78-4 (March 1978).

4. Personal communication, H. Tomlinson, G. O. Carlson, Inc., to D. T. Raske, Argonne National Laboratory (October 1982).

5. Oak Ridge National Laboratory, Mechanical Properties Design Data Program: Semiannual Progress Report for Period Ending January 31, 1983, ORNL/MSP/1.3-83/1, pp. 1-1 to 1-8 (April 1983).

6. American Society of Mechanical Engineers, ASME Boiler and Pressure Vessel Code Case N47-15 (1979).

7. Oak Ridge National Laboratory, Mechanical Properties Design Data Program: Semiannual Progress Report for Period Ending July 31, 1980, ORNL/MSP/1.3-80/2, pp. 2-1 to 2-7 (December 1980).

8. Oak Ridge National Laboratory, Mechanical Properties Design Data Program: Semiannual Progress Report for Period Ending July 31, 1981, ORNL/MSP/1.3-81/3, pp. 1-13 to 1-18 (November 1981).

9. Oak Ridge National Laboratory, Mechanical Properties Design Data Program: Semiannual Progress Report for Period Ending January 31, 1982, ORNL/MSP/1.3-82/1, pp. 4-28 to 4-32 (May 1982).

10. Oak Ridge National Laboratory, Mechanical Properties Design Data Program: Structural Materials Semiannual Progress Report for Period Ending July 31, 1982, ORNL/MSP/1.3-82/3, pp. 1-1 to 1-13 (October 1982).

11. D. T. Raske, Effects of Metallurgical Variables on the Low-Cycle Fatigue and Cyclic Creep-Fatigue Behavior of Type 316 Stainless Steel, Argonne National Laboratory Report ANL-83-12 (April 1983).

12. D. T. Raske, Cyclic-Deformation Resistance of Weld-Deposited Type 16-8-2 Stainless Steel at 593°C, Argonne National Laboratory Report ANL-77-72 (August 1977).

13. Oak Ridge National Laboratory, National Program Plan for Mechanical Properties Design Data, ORNL/MSP/1.3-82/2, Draft, pp. 2-35 (November 1982).

APPENDIX A

DETERMINATION OF THE STRAIN-LIFE CORRELATION BY REGRESSION ANALYSIS

The curves shown in Figs. 6, 7, 9, and 10 are described by a relation between total strain range, $\Delta\varepsilon_t$ (%), and cycles to failure, N_f, of the form

$$\Delta\varepsilon_t(\%) = \alpha_0(\log_{10} N_f)^{\alpha_1} + \alpha_2. \qquad \text{(A-1)}$$

This relation is the inverse of the least-squares regression analysis model used to correlate the data,

$$\log_{10}(\log_{10} N_f) = \beta_0 + \beta_1 \log_{10}(\Delta\varepsilon_t + \beta_2) . \qquad \text{(A-2)}$$

The relationships between the parameters of Eqs. (A-1) and (A-2) are

$$\alpha_0 = 10^{-\beta_0/\beta_1},$$

$$\alpha_1 = 1/\beta_1, \qquad \text{(A-3)}$$

$$\alpha_2 = -\beta_2.$$

Values of these parameters for both the baseline and design curves are summarized in Table A-I. To distinguish between the coarse- and fine-grained high-cycle data, an indicator variable[A1] was used with the β_2 term in the regression analysis model (this term is actually an "endurance limit" strain range). Thus, the β_2 term would have two different values, depending on the grain size. The regression analysis coefficients of determination (R^2) for the baseline data are 0.992 at 482°C and 0.983 at 593°C. Table A.II provides a list of the data used to determine the baseline curves. A fatigue life of 5.31×10^8 cycles for the ANL specimen PU-28 listed in this table was estimated by the iterative least-squares procedure[A2] using the run-out life of 1.03×10^8 cycles (Table II) as the starting value. The procedures converged to the value listed in Table A.II after 6 iterations. The design curves were determined by reducing the baseline curves by a factor of 2 for the strain range or 20 for the fatigue life (whichever resulted in the lowest curve) and then refitting these design data with the regression analysis model.

Figure A.1 shows a plot of the regression analysis residual terms,* N_E, versus the predicted fatigue life (transformed) for the 593°C data. The uniform distribution of the residuals in this plot indicates that the regression analysis model (Eq. A-2) adequately describes the data. The dashed horizontal lines represent 1.960 standard deviations (S = 0.0219) of scatter on either side of zero. Similar plots showing the variation of the residuals with heat, heat treatment, and test laboratory are given in Figs. A-2 through A-4. The only obvious trend in these plots

is that shown in Fig. A-3 which indicates that the low-cycle fatigue specimens that were aged prior to testing have a consistently longer fatigue life than predicted by the correlation. This is also illustrated in Table A.III, which lists the 593°C data in order of increasing residual value. Although these aged data have a different mean residual value than the solution-annealed data, their inclusion in the regression analysis model do not effect the values of the high-cycle endurance strain ranges. In addition, it has been demonstrated that the effects of metallurgical variables, such as aging, need not be quantitatively accounted for in low-cycle, continuous cycling strain-life correlations for Type 316 stainless steel.[A3] Figure A.5 shows a plot of the normal distribution z statistic versus the residual values. The straight line in this figure represents a standard normal line for a population with the same variance as the regression analysis model. The close agreement between the data and the normal line indicates that the choice of transformation on the fatigue life is correct and that the results of normal-distribution theory can be used to analyze the data.[A1] Results similar to those above were also obtained for the data generated at 482°C. However, since the data base consisted of the results from only 6 tests, the significance of these results is moot.

---

*The residual term $\bar{N}E$ is equal to the difference between the observed and predicted fatigue lives (loglog N_{fobs}-loglog N_{fpre}).

Table A.I. Values for the Parameters α_i and β_i in Equations A-1 and A-2

Temperature, °C (°F)	Curve (Fig.)	Grain Size, ASTM	Parameter					
			Eq. A-1			Eq. A-2		
			α_0	α_1	α_2	β_0	β_1	β_2
593 (1100)	Baseline (5)	3.2	62.0	-3.55	0.203	0.505	-0.282	-0.203
		5.0	62.0	-3.55	0.232	0.505	-0.282	-0.232
	Design (6)	3.2	4.17	-2.145	0.0727	0.289	-0.466	-0.0727
		5.0	4.17	-2.145	0.0872	0.289	-0.466	-0.0872
482 (900)	Baseline (8)	3.2	85.8	-3.72	0.218	0.520	-0.269	-0.218
	Design (9)	3.2	4.66	-2.170	0.0762	0.308	-0.461	-0.0762

Table A.II. Data[a] Used for Baseline Curves in Figs. 6 and 9.

TYPE 316 SS AT 482 C

OBS	TS	PS	SR	HEAT	HTREAT	LAB	ID	NF	NFP
1	2.98	2.400	0.004	808	SA	BCL	3	265	330
2	2.02	1.480	0.004	808	SA	BCL	4	897	668
3	1.02	0.680	0.004	808	SA	BCL	5	4026	3247
4	0.50	0.250	0.004	808	SA	BCL	6	26938	44690
5	0.26	0.001	.	297	SA	INEL	DR-34	146700000	56342940
6	0.25	0.006	.	297	SA	INEL	DR-7	110200000	216547498

TYPE 316 SS AT 593 C

OBS	TS	PS	SR	HEAT	HTREAT	LAB	ID	NF	NFP
1	3.930	3.300	0.0039	808	SA	ANL	GR2-7	113	162
2	2.050	1.500	0.0040	583	SA	INEL	E2-43	639	492
3	2.000	1.480	0.0040	808	SA	INEL	D-74	406	516
4	2.000	1.430	0.0040	808	SA	INEL	D-139	406	516
5	2.000	1.480	0.0040	808	SA	INEL	D-213	445	516
6	2.000	1.450	0.0040	808	SA	INEL	D-143	450	516
7	2.000	1.450	0.0040	808	SA	INEL	D-223	547	516
8	2.000	1.480	0.0040	808	AGED	INEL	D-79	581	516
9	2.000	1.510	0.0040	808	AGED	INEL	D-77	608	516
10	2.000	1.530	0.0040	808	AGED	INEL	D-43	671	516
11	2.000	1.580	0.0040	808	AGED	INEL	D-226	914	516
12	1.980	1.570	0.0040	808	AGED	INEL	D-251	534	526
13	1.020	0.590	0.0040	808	SA	INEL	D-146	2241	2441
14	1.010	0.640	0.0040	808	AGED	INEL	D-45	4000	2508
15	1.000	0.560	0.0040	808	SA	INEL	D-148	2040	2578
16	1.000	0.580	0.0040	808	SA	INEL	D-214	2213	2578
17	1.000	0.620	0.0040	583	SA	INEL	E2-50	2308	2578
18	1.000	0.630	0.0040	808	AGED	INEL	D-215	2773	2578
19	1.000	0.580	0.0040	808	AGED	INEL	D-81	3266	2578
20	0.990	0.640	0.0040	808	AGED	INEL	D-225	2603	2651
21	0.980	0.530	0.0040	808	AGED	INEL	D-36	2962	2728
22	0.900	0.510	0.0040	583	SA	INEL	E2-42	3512	3489
23	0.780	0.450	0.0040	808	AGED	INEL	D-239	8334	5450
24	0.670	0.360	0.0130	297	SA	ANL	PU-14	9860	9246
25	0.620	0.230	0.0040	583	SA	INEL	E2-38	9092	12433
26	0.510	0.230	0.0040	583	SA	INEL	E2-44	10780	29088
27	0.510	0.200	0.0040	808	AGED	INEL	D-88	42947	29088
28	0.510	0.210	0.0040	808	AGED	INEL	D-78	56671	29088
29	0.500	0.220	0.0040	808	SA	INEL	D-147	24850	32032
30	0.500	0.200	0.0040	808	SA	INEL	D-193	27898	32032
31	0.500	0.190	0.0040	808	SA	INEL	D-150	29822	32032
32	0.490	0.210	0.0040	808	AGED	INEL	D-216	106622	35423
33	0.420	0.190	0.0040	583	SA	INEL	E2-47	32969	83614
34	0.350	0.080	0.0040	808	SA	ANL	GR4-1	91773	311427
35	0.330	0.019	0.0066	297	SA	ANL	PU-17	980000	1416632
36	0.330	0.020	0.0066	297	SA	ANL	PU-42	3568000	1416632
37	0.330	0.022	0.0066	297	SA	ANL	PU-24	5086000	1416632
38	0.329	0.036	0.0011	297	SA	ANL	PU-12	787000	1475671
39	0.300	0.017	0.0040	297	SA	ANL	PU-8	6610000	6532502
40	0.280	0.003	.	297	SA	ANL	PU-48	14870000	32560338
41	0.280	0.004	.	297	SA	ANL	PU-46	35350000	32560338
42	0.280	0.003	.	297	SA	ANL	PU-26	68310000	32560338
43	0.260	0.003	.	297	SA	ANL	PU-28	531000000	537132568
44	0.290	0.013	.	297	SA	ANL	PU-30LGS	3067000	2336132
45	0.400	0.100	0.0040	297	SA	BCL	A33	33500	114359
46	0.337	0.034	0.0040	297	SA	BCL	A34	180170	435108
47	0.350	0.043	0.0040	297	SA	INEL	DR-6	243397	311427
48	0.330	0.047	.	297	SA	INEL	DR-39	238790	530282
49	0.330	0.027	0.0066	297	SA	INEL	DR-31	426497	530282
50	0.330	0.008	0.0066	297	SA	INEL	DR-38	1155246	530282
51	0.320	0.023	0.0040	297	SA	INEL	DR-9	910898	721709
52	0.310	.	0.0062	297	SA	INEL	DR-52	698989	1017998
53	0.290	0.026	.	297	SA	INEL	DR-27	1675317	2336132
54	0.280	0.008	.	297	SA	INEL	DR-53	2833816	3903440
55	0.280	0.006	.	297	SA	INEL	DR-55	7292166	3903440
56	0.280	0.013	.	297	SA	INEL	DR-22	8750310	3903440
57	0.28	0.007	0.0056	297	SA	INEL	DR-33	19320150	3903440
58	0.27	0.001	0.0054	297	SA	INEL	DR-56	16882900	7161019
59	0.26	0.014	.	297	SA	INEL	DR-24	10775485	14942609
60	0.25	0.007	.	297	SA	INEL	DR-29	31191233	37599210
61	0.24	0.006	.	297	SA	INEL	DR-35	62012310	126868816
62	0.24	0.007	.	297	SA	INEL	DR-13	134860380	126868816
63	0.29	0.008	.	297	SA	INEL	DRA-2SGS	18927785	13349411
64	0.28	0.002	.	297	SA	INEL	DRA-1SGS	12814000	32560338
65	0.35	.	0.0070	297	SA	RNL	KD1	225000	311427
66	0.31	.	0.0062	297	SA	RNL	KD2	5510000	1017998

[a] TS = total strain range, %; PS = plastic strain range, %; SR = strain rate, s^{-1}, Heat 808 - 65808, Heat 583 = 81583, Heat 297 = 8092297, HTREAT = heat treatment, SA = solution annealed, AGED = aged prior to testing, ANL = Argonne National Laboratory, BCL = Battelle Columbus Laboratories, INEL = Idaho National Engineering Laboratory, RNL = Risley Nuclear Power Development Laboratories (UK), ID = specimen identification, NF = actual cycles to failure, and NFP = predicted cycles to failure.

Table A.III. Data[a] Used for Baseline Curve in Fig. 6 in Order of Increasing Residual Value

TYPE 316 SS AT 593 C

OBS	N_E	TS	PS	SR	HEAT	HTREAT	LAB	ID	NF	NFP
1	-0.048379	0.400	0.100	0.0040	297	SA	BCL	A33	33500	114359
2	-0.044118	0.350	0.080	0.0040	808	SA	ANL	GR4-1	91773	311427
3	-0.044110	0.510	0.230	0.0040	583	SA	INEL	E2-44	10780	29088
4	-0.037210	0.420	0.190	0.0040	583	SA	INEL	E2-47	32969	83614
5	-0.031685	3.930	3.300	0.0039	808	SA	ANL	GR2-7	113	162
6	-0.030542	0.337	0.034	0.0040	297	SA	BCL	A34	180170	435108
7	-0.027116	0.330	0.047	.	297	SA	INEL	DR-39	238790	530282
8	-0.024067	0.280	0.002	.	297	SA	INEL	DRA-1SGS	12814000	32560338
9	-0.020136	0.280	0.003	.	297	SA	ANL	PU-48	14870000	32560338
10	-0.019658	0.329	0.036	0.0011	297	SA	ANL	PU-12	787000	1475671
11	-0.016996	2.000	1.480	0.0040	808	SA	INEL	D-74	406	516
12	-0.016996	2.000	1.430	0.0040	808	SA	INEL	D-139	406	516
13	-0.016989	0.240	0.006	.	297	SA	INEL	DR-35	62012310	126868816
14	-0.014662	0.620	0.230	0.0040	583	SA	INEL	E2-38	9092	12433
15	-0.013136	1.000	0.560	0.0040	808	SA	INEL	D-148	2040	2578
16	-0.011966	0.310	.	0.0062	297	SA	INEL	DR-52	698989	1017998
17	-0.011448	0.330	0.019	0.0066	297	SA	ANL	PU-17	980000	1416632
18	-0.011307	0.350	.	0.0070	297	SA	RNL	KD1	225000	311427
19	-0.010760	0.500	0.220	0.0040	808	SA	INEL	D-147	24850	32032
20	-0.010414	2.000	1.480	0.0040	808	SA	INEL	D-213	445	516
21	-0.009961	0.290	0.026	.	297	SA	INEL	DR-27	1675317	2336132
22	-0.009619	2.000	1.450	0.0040	808	SA	INEL	D-143	450	516
23	-0.009261	0.280	0.008	.	297	SA	INEL	DR-53	2833816	3903440
24	-0.008681	0.260	0.014	.	297	SA	INEL	DR-24	10775485	14942609
25	-0.008546	0.350	0.043	0.0040	297	SA	INEL	DR-6	243397	311427
26	-0.008522	1.000	0.580	0.0040	808	SA	INEL	D-214	2213	2578
27	-0.007236	0.330	0.027	0.0066	297	SA	INEL	DR-31	426497	530282
28	-0.006159	1.000	0.620	0.0040	583	SA	INEL	E2-50	2308	2578
29	-0.005823	0.500	0.200	0.0040	808	SA	INEL	D-193	27898	32032
30	-0.004780	1.020	0.590	0.0040	808	SA	INEL	D-146	2241	2441
31	-0.004677	0.250	0.007	.	297	SA	INEL	DR-29	31191233	37599210
32	-0.003003	0.500	0.190	0.0040	808	SA	INEL	D-150	29822	32032
33	-0.001010	0.990	0.640	0.0040	808	AGED	INEL	D-225	2603	2651
34	-0.000248	0.260	0.003	.	297	SA	ANL	PU-28	531000000	537132568
35	0.000326	0.300	0.017	0.0040	297	SA	ANL	PU-8	6610000	6532502
36	0.000356	0.900	0.510	0.0040	583	SA	INEL	E2-42	3512	3489
37	0.001010	1.980	1.570	0.0040	808	AGED	INEL	D-251	534	526
38	0.001420	0.240	0.007	.	297	SA	INEL	DR-13	134860380	126868816
39	0.002059	0.280	0.004	.	297	SA	ANL	PU-46	35350000	32560338
40	0.003046	0.670	0.360	0.0130	297	SA	ANL	PU-14	9860	9246
41	0.004015	1.000	0.630	0.0040	808	AGED	INEL	D-215	2773	2578
42	0.004041	2.000	1.450	0.0040	808	SA	INEL	D-223	547	516
43	0.004501	0.980	0.530	0.0040	808	AGED	INEL	D-36	2962	2728
44	0.007431	0.320	0.023	0.0040	297	SA	INEL	DR-9	910898	721709
45	0.007988	0.290	0.013	.	297	SA	ANL	PU-30LGS	3067000	2336132
46	0.008175	2.000	1.480	0.0040	808	AGED	INEL	D-79	581	516
47	0.009145	0.290	0.008	.	297	SA	INEL	DRA-2SGS	18927785	13349411
48	0.011263	2.000	1.510	0.0040	808	AGED	INEL	D-77	608	516
49	0.012888	1.000	0.580	0.0040	808	AGED	INEL	D-81	3266	2578
50	0.016159	0.510	0.200	0.0040	808	AGED	INEL	D-88	42947	29088
51	0.017524	0.280	0.006	.	297	SA	INEL	DR-55	7292166	3903440
52	0.017892	2.000	1.530	0.0040	808	AGED	INEL	D-43	671	516
53	0.017979	2.050	1.500	0.0040	583	SA	INEL	E2-43	639	492
54	0.018215	0.280	0.003	.	297	SA	ANL	PU-26	68310000	32560338
55	0.020924	0.780	0.450	0.0040	808	AGED	INEL	D-239	8334	5450
56	0.022505	0.280	0.013	.	297	SA	INEL	DR-22	8750310	3903440
57	0.0229791	0.27	0.001	0.0054	297	SA	INEL	DR-56	16882900	7161019
58	0.0249262	0.33	0.008	0.0066	297	SA	INEL	DR-38	1155246	530282
59	0.0251615	1.01	0.640	0.0040	808	AGED	INEL	D-45	4000	2508
60	0.0273038	0.51	0.210	0.0040	808	AGED	INEL	D-78	56671	29088
61	0.0274382	0.33	0.020	0.0066	297	SA	ANL	PU-42	3568000	1416632
62	0.0375241	0.33	0.022	0.0066	297	SA	ANL	PU-24	5086000	1416632
63	0.0380397	2.00	1.580	0.0040	808	AGED	INEL	D-226	914	516
64	0.0434389	0.49	0.210	0.0040	808	AGED	INEL	D-216	106622	35423
65	0.0435090	0.28	0.007	0.0056	297	SA	INEL	DR-33	19320150	3903440
66	0.0500225	0.31	.	0.0062	297	SA	RNL	KD2	5510000	1017998

[a] N_E = residual value, TS = total strain range, %; PS = plastic strain range, %; SR = strain rate, s^{-1}, Heat 808 = 65808, Heat 583 = 81583, Heat 297 = 8092297, HTREAT = heat treatment, SA = solution annealed, AGED = aged prior to testing, ANL = Argonne National Laboratory, BCL = Battelle Columbus Laboratories, INEL = Idaho National Engineering Laboratory, RNL = Risley Nuclear Power Development Laboratories (UK), ID = specimen identification, NF = actual cycles to failure, and NFP = predicted cycles to failure.

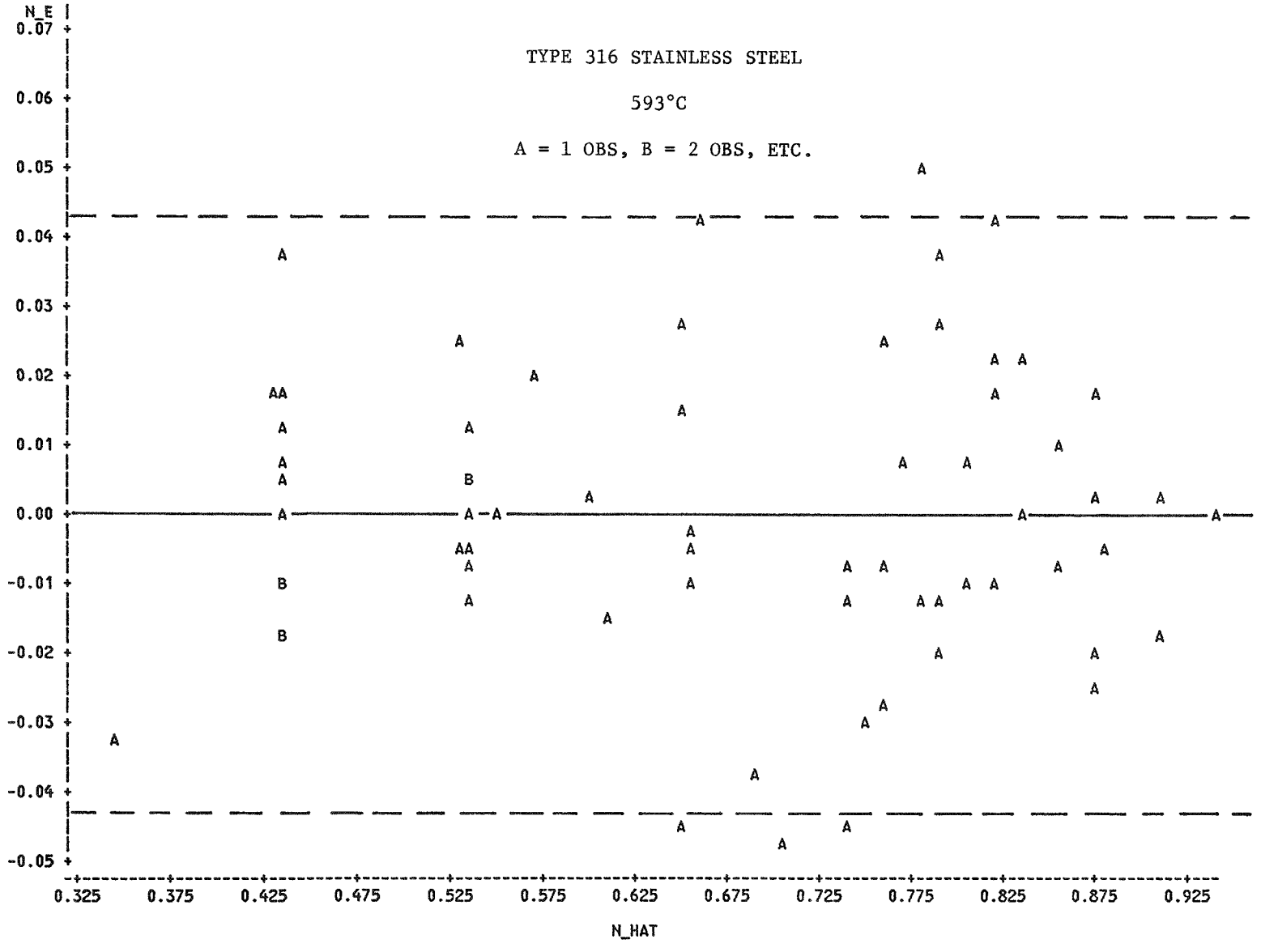

Fig. A.1. Residual Values (N_E) vs. Predicted Fatigue Life (N_HAT).

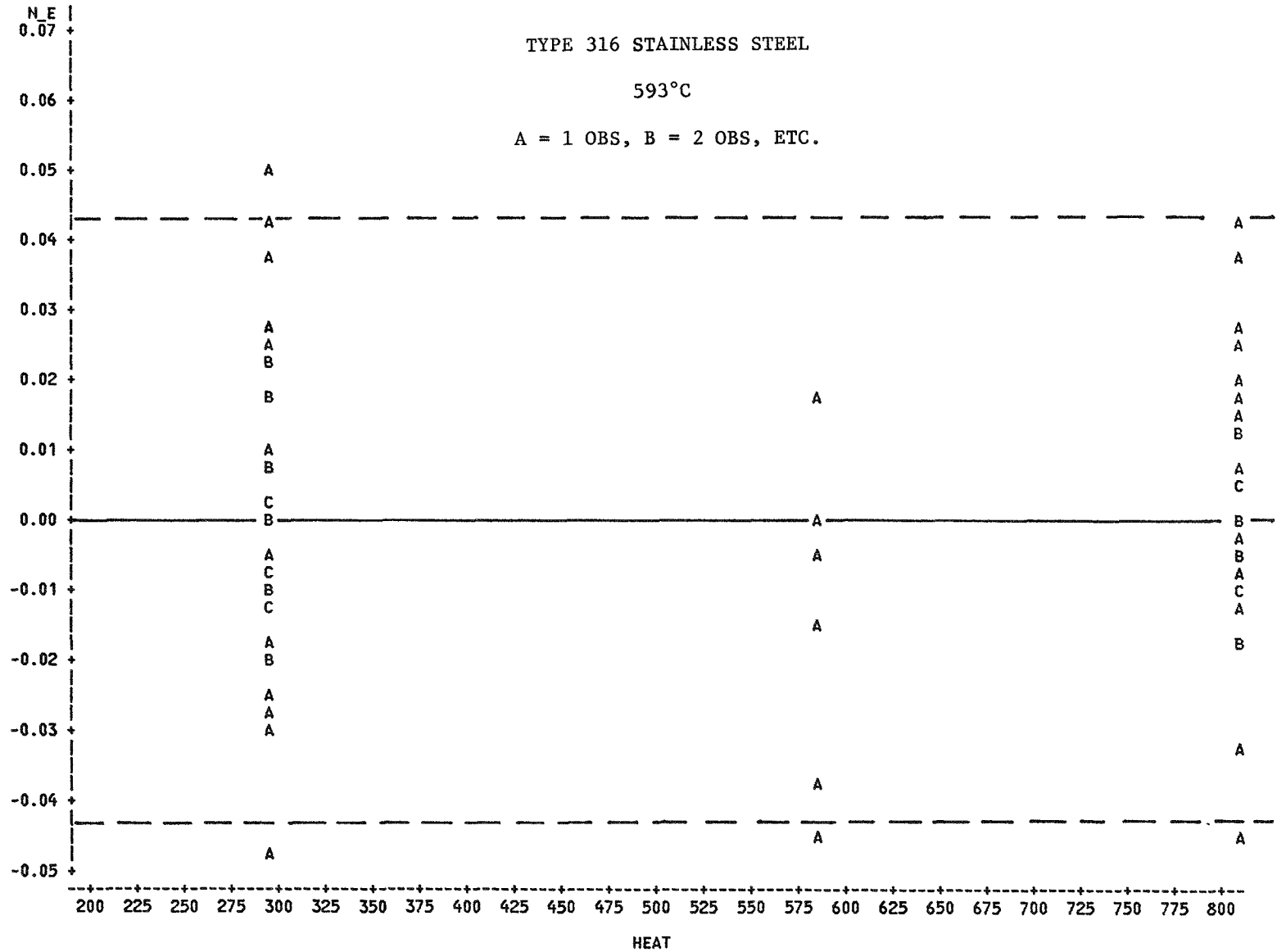

Fig. A.2. Residual Values (N_E) vs. Heat.

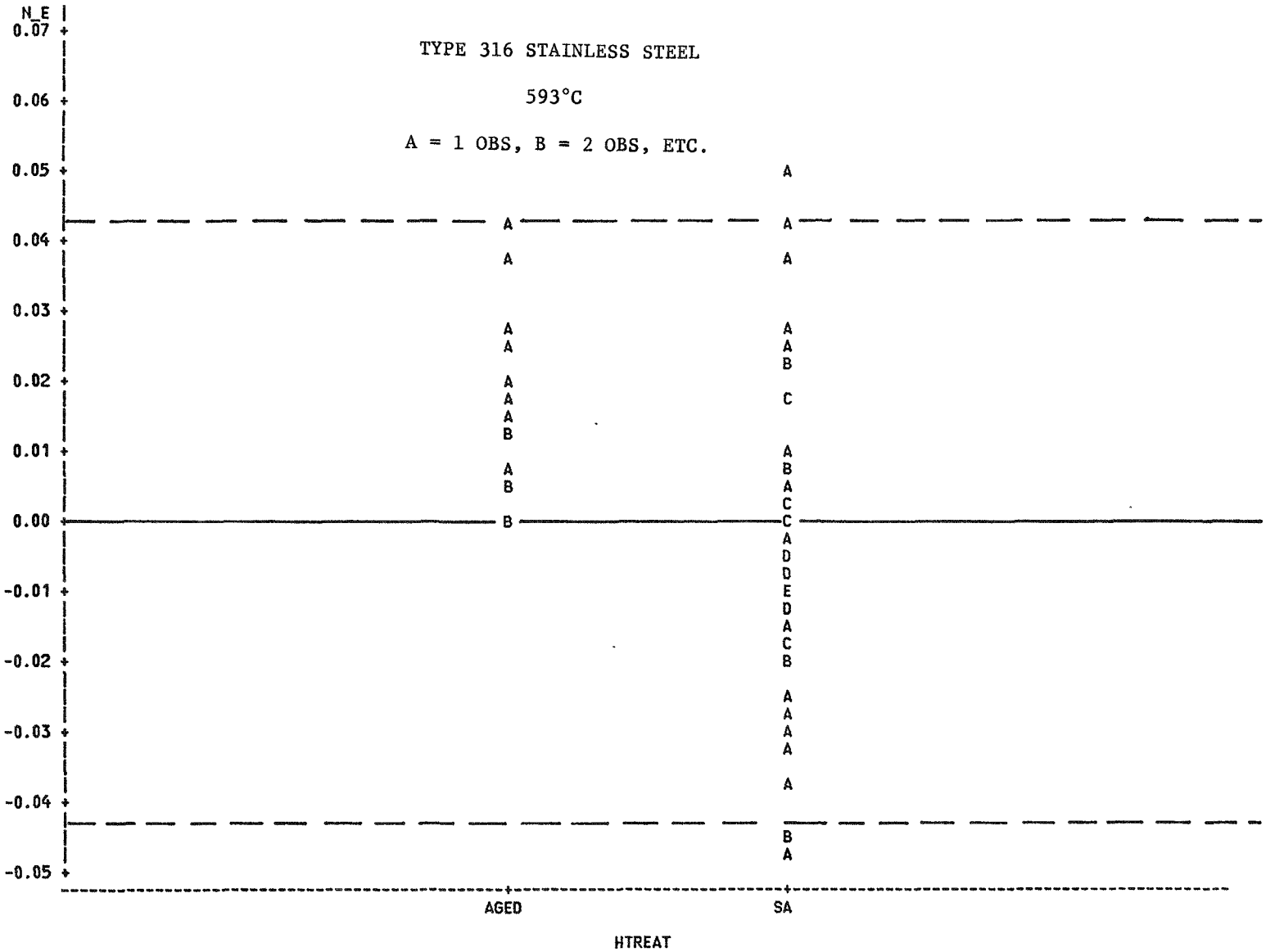

Fig. A.3. Residual Values (N_E) vs. Heat-treatment (HTREAT).

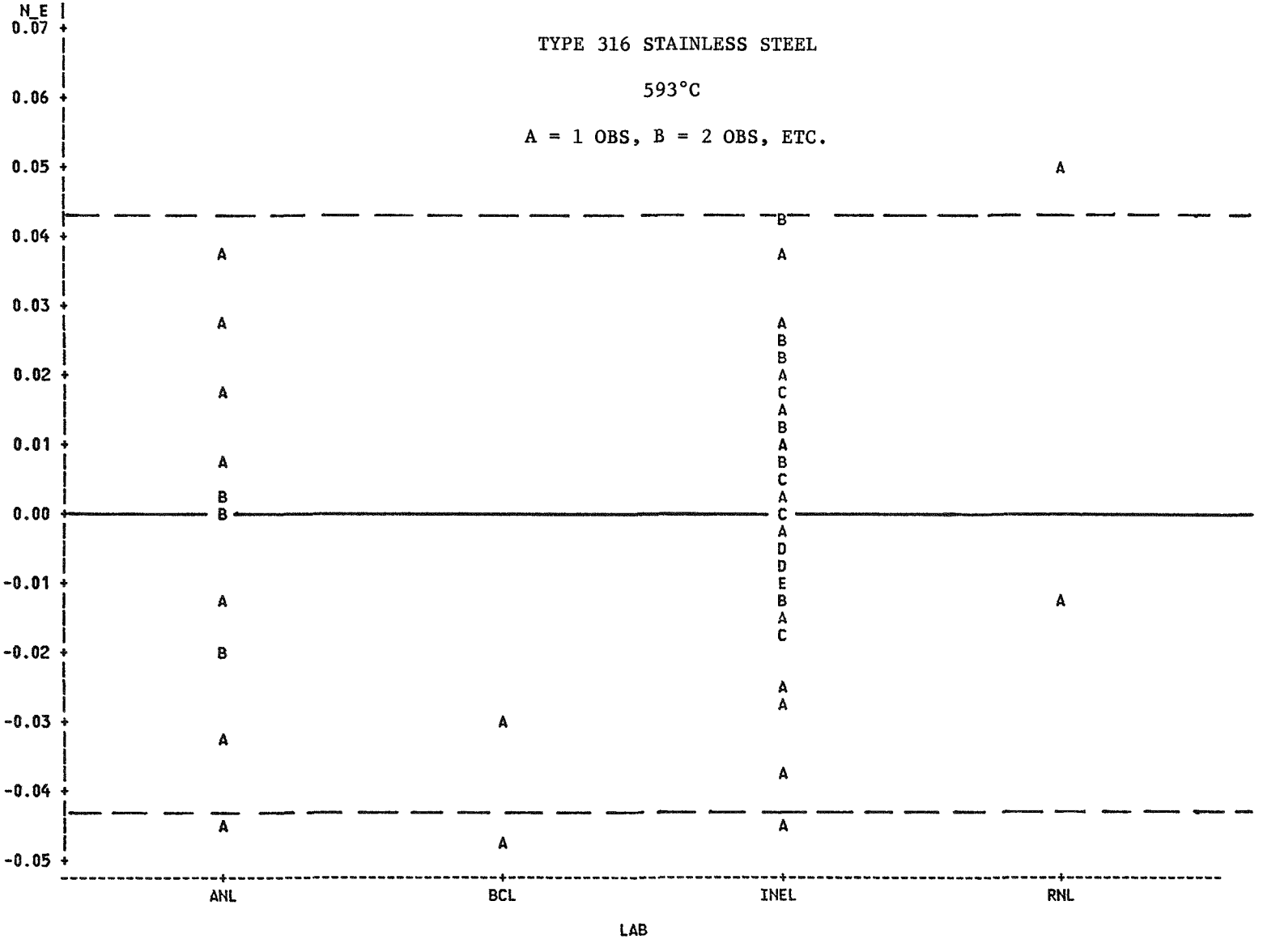

Fig. A.4. Residual Value (N_E) vs. Testing Laboratory (LAB).

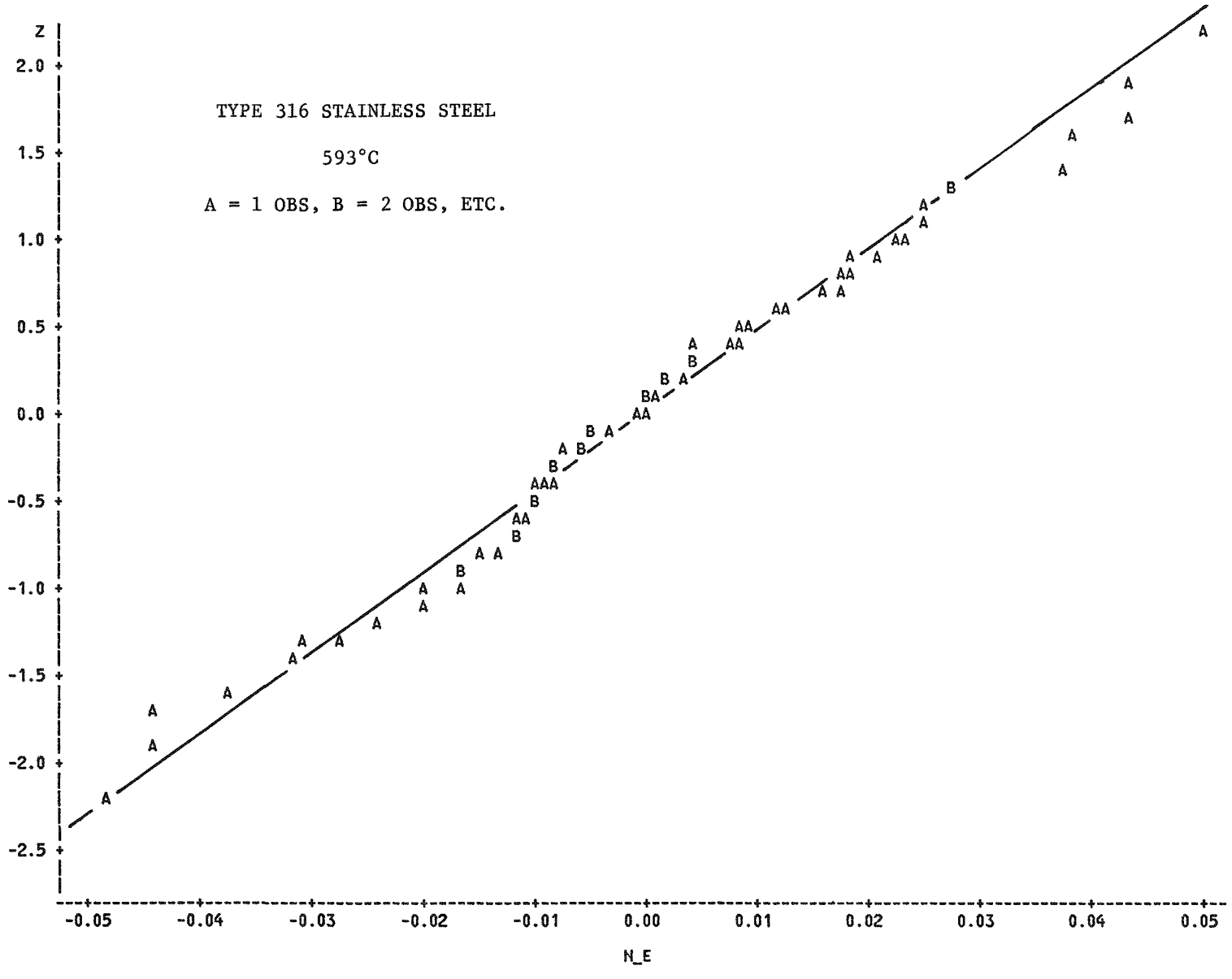

Fig. A.5. Normal Distribution Statistic (Z) vs. Residual Value (N_E).

REFERENCES

A1. J. Neter and W. Wasserman, Applied Linear Statistical Models, Richard D. Irwin, Inc. (1974).

A2. J. Schmee and G. J. Hahn, "A Simple Method for Regression Analysis with Censored Data," Technometrics 21(4):417-432 (1979).

A3. D. T. Raske, The Effect of Metallurgical Variables on the Low-Cycle Fatigue and Cyclic Creep-Fatigue Behavior of Type 316 Stainless Steel, Argonne National Laboratory Report ANL-83-12 (April 1983).

Distribution for ANL-83-35

Internal:

E. S. Beckjord
C. E. Till
R. Avery
B. R. T. Frost
K. L. Kliewer
R. A. Lewis
R. S. Zeno
R. W. Weeks
E. M. Stefanski
W. J. Shack
A. G. Hins
T. F. Kassner
P. S. Maiya
D. R. Diercks
J. C. Tezak
J. Y. Park
F. A. Nichols
D. E. Busch
W. F. Burke
S. Majumdar
D. T. Raske (20)
K. J. Reimann
H. R. Thresh
ANL Patent Dept.
ANL Contract File
ANL Libraries (2)
TIS Files (3)

External:

DOE-TIC, for distribution per UC-79Th (131)
Manager, Chicago Operations Office, DOE
Director, Technology Management Div., DOE-CH
Director, Breeder Technology Projects, DOE-Wash. (2)
Materials Science and Technology Division Review Committee:
C. B. Alcock, U. Toronto
A. Arrott, Simon Fraser U.
R. C. Dynes, Bell Labs., Murray Hill
A. G. Evans, U. California, Berkeley
L. M. Falicov, U. California, Berkeley
H. K. Forsen, Bechtel Group, Inc., San Francisco
E. Kay, IBM San Jose Research Lab.
M. B. Maple, U. California--San Diego
P. G. Shewmon, Ohio State U.
J. K. Tien, Columbia U.